

# ADVENT OF SUPERCONDUCTIVITY AND SUBSTITUTIONAL STUDIES IN YBCO SUPERCONDUCTORS

*by*

ANAND K. TYAGI

TH  
IPMS/1990/14  
Ty 959

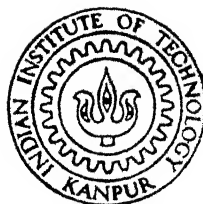
IPMS

1990

M

TYA

ADV



Interdisciplinary Programme in Materials Science

INDIAN INSTITUTE OF TECHNOLOGY KANPUR

1990

*ADVENT OF SUPERCONDUCTIVITY  
AND SUBSTITUTIONAL STUDIES  
IN YBCO SUPERCONDUCTORS*

*A Dissertatlion submltted  
as project work for the degree of  
MASTER OF TECHNOLOGY*

*By*

*ANAND K. TYAGI*

*To the*

*INTERDISCIPLINARY PROGRAMME IN MATERIALS SCIENCE  
INDIAN INSTITUTE OF TECHNOLOGY  
KANPUR*

MS-1990-M-TYA-ADV

18 SEP 1990

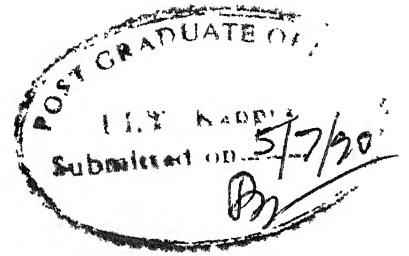
ENTRAL LIBRARY  
U. S. KANGOR

Ac. No. A.108883

To  
my baby girl  
T.Amrita Rupasi



CERTIFICATE



Certified that this dissertation "ADVENT OF SUPERCONDUCTIVITY AND SUBSTITUTIONAL STUDIES IN YBCO SUPERCONDUCTORS" is being submitted to Indian Institute of Technology Kanpur as PROJECT WORK for the award of the degree of MASTER OF TECHNOLOGY in MATERIALS SCIENCE. This work has been completed by Sh. ANAND KUMAR TYAGI under my supervision and has not been submitted elsewhere for a degree.

*KShah*

( Keshav Shah )

Assistant Professor  
ACMS, IIT Kanpur-208016

July ,1990

## CONTENTS

	Page
CHAPTER 1	
Introduction	
1.1    Brief History of Superconductivity	1
1.2    The Signatures of the Superconducting State	3
1.21    Loss of Resistivity	3
1.22    Abrupt Change in Specific Heat	5
1.23    The Abrupt Change in Thermoelectric Power	7
1.24    Perfect Diamagnetism in Superconductors Abrupt Change in Magnetic Susceptibility	9
1.25    Characteristic Change in Microwave Absorption	11
1.3    Current Theoretical Status in High T <sub>c</sub> Superconductivity	13
1.31    BCS Type Theories	14
1.32    Bose Condensation Type Theories	16
1.4    Crystal Structure of YBCO High Temperature Superconductors.	18
1.41    Role of Oxygen	20
1.42    Role of Copper in Superconductivity	21
1.5    Substitutional Studies in YBCO Superconductors	22
1.51    Substitutions at Cu-Sites	24
1.52    Substitutions at Oxygen Site	26
1.6    Statement of Problem	27

	Page
Tables	29
Figures	38
References	41
 CHAPTER 2	
Experimental Techniques	
2.1 Methodologies for Materials Preparation	49
2.11 Pseudoternary Phase diagram of $Y_2O_3$ -BaO-CuO System	49
2.12 Sample Preparation	50
2.2 Materials Characterization	52
2.21 X-Ray Diffraction (XRD)	52
2.22 Scanning Electron Microscopy - EDX Measurements	53
2.23 Resistivity Measurements	54
Tables	59
Figures	60
References	64
 CHAPTER 3	
Results and Discussion	
3.1 X-Ray Diffraction (XRD)	65
3.2 Scanning Electron Microscopy (SEM)-EDX Analysis	69
3.3 Resistivity Measurements	72
Conclusions	77
Tables	78
Figures	86
Plates	96
References	98

## LIST OF TABLES

	Page
1.1 Some representative superconducting elements	29
1.2 Superconducting transition temperatures ( $T_c$ ) and critical fields ( $H_c$ ) for some representative alloys and intermetallics	30
1.3 High temperature oxide superconductors	31
1.4 Some of the pairing mechanisms in high temperature superconductors	33
1.5 Comparison of salient features of superconducting cuprates.	34
1.6 Cationic/Anionic substitutions in YBCO high temperature superconductors	35
2.1 The preparational details of PbS doped YBCO samples	59
3.1 X-Ray powder diffraction data for $YBa_2(Cu_{1-x}Pb_x)_3S_{3-x}O_y$	78
3.2 Relative intensities of main impurity phases as a function of doping	82
3.3 Room temperature resistivities ( $\rho_{300}$ ), transition temperatures ( $T_c$ ) and transition widths ( $\Delta T_c$ ) for superconducting oxides $YBa_2(Cu_{1-x}Pb_x)_3S_{3-x}O_y$	84
3.4 Superconducting order parameter and characteristic length parameter as a function of doping ( $x$ ) in $YBa_2(Cu_{1-x}Pb_x)_3S_{3-x}O_y$ .	85

## LIST OF FIGURES

### Page

1.1	Chronology of events and Hallmark developments in superconductivity research.	38
1.2	Signatures of superconducting state and their consequences	39
1.3	Structures of $\text{YBa}_2\text{Cu}_3\text{O}_{7-\delta}$	40
2.1	Pseudoternary phasediagram of the $\text{Y}_2\text{O}_3\text{BaO-CuO}$ system	60
2.2	$\text{CuO-X}$ and $\text{BaCuO}_2\text{-Y}$ Vertical sections of $\text{BaCuO}_2\text{-211-CuO}$ triangle in YBCO Pseudoternary phase diagram	61
2.3	Dependence of effective thickness $d_{\text{eff}}$ on probe-distances $l_1$ and $l_2$	62
2.4	Simplified expander module diagram	63
3.1	X-Ray Diffraction patterns for $\text{YBa}_2(\text{Cu}_{1-x}\text{Pb}_x)_3\text{S}_{3-x}\text{O}_y$	86
3.2	EDX-spectrum of pure Ortho-phase showing its chemical composition $\text{YBa}_2\text{Cu}_3\text{O}_7$	87
3.3	EDX-spectrum of a portion of PbS-doped YBCO specimen showing an impurity phase of nominal composition $\text{Y}_2\text{BaCuO}_5$	88
3.4	EDX-spectrum showing the second (gray) impurity phase rich in Ba and Cu	89
3.5	EDX-spectrum showing the second impurity phase rich in Ba and Pb, having composition very near to $\text{BaPbO}_3$	90
3.6.	Normalized Resistivity vs. Temperature plots for PbS doped YBCO.	91
3.7	Transition regions of the PbS doped YBCO-superconductors	92

	Page
3.8 Derivative $d\rho/dT$ vs. Temperature for PbS doped YBCO	93
3.9 Paraconductivity vs. Reduced temperature for PbS doped YBCO	94
3.10 Characteristic parameters for PbS doped YBCO high $T_c$ superconductor.	95

## LIST OF PLATES

Page

- |     |                                                                                          |    |
|-----|------------------------------------------------------------------------------------------|----|
| 3.1 | SEM-Microphotograph for the sample AK02T ( $x=0$ )                                       | 96 |
| 3.2 | SEM-Microphotograph for the sample AK11T ( $x=0.02$ ) showing an increase in grain size. | 96 |
| 3.3 | SEM-Microphotograph for the sample AK02T ( $x=0.05$ )                                    | 97 |
| 3.4 | SEM-Microphotograph for the sample AK17T ( $x=0.02$ ) showing a reduction in grain size. | 97 |

## ACKNOWLEDGEMENT

I am extremely grateful to Dr. K. Shahi, A.P., Materials Science Programme, IIT Kanpur, under whose supervision this dissertation has been completed. I had the privilege of his constant guidance during this project work. I am also thankful to Dr. D.C. Agrawal, Head, M.S.P., Dr. S.D. Tyagi, Drexel University, USA and my father Sh. R.N. Tyagi for their ceaseless inspiration through out the course of the present work.

My profound regards are due to Dr. R. Raj Kumar, Sh. S.J. Raina, Dr. N.K. Jain, Dr. S.K. Handoo, Sh. S.C. Sharma and Dr. S. Harsh for their kind co-operation and encouragement.

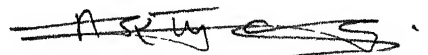
I wish to place on record my deep thanks to S/Sh. Uma Shanker, P.K. Pal, U.S. Lal, B. Sharma and B.K. Jain for their technical contributions.

Heartful thanks are due to Ajay, Ashok, Kulvir, Manoravi, Shiuli, Ajay Garg, Satyaveer, Manvendra, Suman, Sujata, Padamanabhan and M. Roy, who helped me in this work directly or indirectly.

I am also grateful to S/Sh. D.N. Sharma and R.P. Vijayavergia for their kind help in my domestic problems.

Sincere thanks are also due to my mother Smt.. Snehlata for her influential encouragement. My cordial thanks are also due to my wife Deosuta for her support and valuable comments. I also dare to get excused of seizing the time from the moments of affection of my baby girl T. Amrita Rupasi during the period of this work.

Thanks are also due to Sh. J. Singh for the excellent typing of this dissertation.

  
( Anand K. Tyagi )

July 1990.



## CHAPTER - 1

### 1. INTRODUCTION

Following the recent discoveries of high  $T_c$  oxide superconductors, an unprecedented research and development effort has been launched worldwide to develop new materials with higher  $T_c$  and better superconducting properties, as well as to explore the possibility of their application in new technologies. The enthusiasm in general has been so great that even a common-man has been following the striking achievements in last four years<sup>1-4</sup>. However, it is only an understanding of the basic principles<sup>6-15</sup> that can help us appreciate the real extent of extraordinary achievements of the last few years..

#### 1.1 Brief History of Superconductivity

Superconductivity is a phenomenon wherein the d.c. electrical resistivity of a material becomes zero or drops by many orders of magnitude to be vanishingly small, contrary to usual behavior, as the material is cooled down. The phenomenon was first observed by Onnes<sup>16</sup> who found that mercury becomes superconducting at 4.2K. Subsequently many metallic elements and alloys were found to superconduct at ambient pressures and several more do when placed under high pressures<sup>17</sup>. Some representative superconducting elements and alloys are listed in Table 1.1 and 1.2 respectively.

The discovery of superconducting transition temperature ( $T_c$ ) above 10K in NbC and NbN was a break through. The invention

of Al<sub>5</sub> compounds, with T<sub>c</sub> finally breaking through the 20K barrier in late 1960,s and early 1970's, represents the culmination of two decades of intense research for higher T<sub>c</sub>. The later, efforts for increasing T<sub>c</sub> mainly concentrated on intermetallic compounds (Table 1.2). With a T<sub>c</sub> of 23.3 in Nb<sub>3</sub>Ge, however, an upper limit of T<sub>c</sub> seemed to have been approached and reports of materials with higher T<sub>c</sub> appeared only occasionally.

A major break-through in the field of superconductivity was reported by Bednorz and Muller <sup>1</sup> who found the evidence of a superconducting transition near 30K in LaBaCuO ternary oxide. It was established later that T<sub>c</sub> in the range 20-40K occurs for La<sub>2-x</sub>M<sub>x</sub>CuO<sub>4-y</sub> (LMCO) with M=Ba,Sr,Ca and that application of pressure, drives T<sub>c</sub> above 50K in Sr. System.

Since pressure was found very effective in increasing the T<sub>c</sub> for La<sub>2-x</sub>Sr<sub>x</sub>CuO<sub>4-y</sub> (LSCO) system, Wu et al <sup>2</sup> simulated chemical pressure by replacing atoms in the LMCO system by smaller isovalent ones. The replacement of La by Y in LBCO produced in early 1987, a 90K superconductor, later identified as YBa<sub>2</sub>Cu<sub>3</sub>O<sub>7-δ</sub> (YBCO). Although there were numerous reports of resistive and magnetic anomalies at much higher temperatures, the next significant discovery, was made in early 1988 by Maeda et al <sup>3</sup> and Chu et al <sup>18</sup> who found a higher T<sub>c</sub> in Bi<sub>2</sub>Sr<sub>2</sub>CaCu<sub>2</sub>O<sub>8-δ</sub> (denoted as Bi 2212 or BSCCO). This was followed rapidly by a catastrophic enhancement in T<sub>c</sub>. Sheng and Herman<sup>4</sup> reported on a high T<sub>c</sub> phase in Tl-Sr-ca-Cu-O system. The superconductor Tl<sub>2</sub>Ba<sub>2</sub>Ca<sub>2</sub>Cu<sub>3</sub>O<sub>10</sub> [Tl-2223] has been found<sup>10,12</sup> to show the highest T<sub>c</sub> (125K) of any known bulk superconductor.

The chronology of events and hallmark developments that led to advancements in high  $T_c$  superconductivity research are diagrammatically represented in Fig. 1.1, Tables 1.4 and 1.5 list the various oxide superconductors and their salient features respectively.

## 1.2 The Signature of the Superconducting State

The superconducting state may be identified by abrupt changes in physical properties of the material, some of the important ones are described below.

### 1.2.1 Loss of Resistivity

An abrupt drop in resistivity of a material at a characteristic temperature ' $T_c$ ' and an apparent absence of resistance to the flow of electricity below  $T_c$  (Fig. 1.2(a)) gives the indication of superconducting state. The complete disappearance of resistivity may be demonstrated by the current which continues to flow without change within the limits of detection, in a superconducting ring placed in a magnetic field changing with time. This current is usually referred to as persistent current.

Experimentally observed rounding off of the resistivity vs. temperature plot just above  $T_c$  has been interpreted frequently as a possible signature of the onset of a higher temperature superconducting phase, but recent studies<sup>21,22</sup> have shown that this effect is a manifestation of thermodynamic superconducting fluctuations above  $T_c$ . The study of this fluctuation phenomena near  $T_c$  is made by observing the excess

conductivity due to superconducting transition at temperatures above  $T_c$ . This excess conductivity is usually called paraconductivity ( $P.SIGMA$ ).

The paraconductivity is the sum of two parts; one is attributable to the direct acceleration of the superconducting pairs created by fluctuations<sup>23</sup> and the other is an indirect effect of fluctuations viz., the superconducting fluctuations decay into pairs of quasi-particles which continue to be accelerated, irrespective of the impurity potential, much as they were, while they were a superconducting fluctuation<sup>24</sup> and this gives an additional contribution to the conductivity. After the completion of life time, these quasi-particles decay back into a superconducting fluctuation.

The first contribution is usually referred to as the direct Aslamazov-Larkin (AL) contribution and the second as the indirect Maki Thomson (MT) contribution. The AL contribution to paraconductivity is usually expressed (depending upon the dimensionality of the material) as<sup>23</sup>

$$\sigma_{3D}^{AL} = [e^2/32.\hbar.\xi(0)]\epsilon^{-1/2} \quad \dots (1)$$

$$\sigma_{2D}^{AL} = [e^2/16.\hbar.d]\epsilon^{-1} \quad \dots (2)$$

$$\sigma_{1D}^{AL} = [e^2.\pi.\xi(0)/16.\hbar.s]\epsilon^{-3/2} \quad \dots (3)$$

where  $\epsilon \equiv$  Reduced temperature  $(T-T_c)/T_c$

$\xi(0) \equiv$  GL Coherence length at  $T = 0$

$d$   $\equiv$  Characteristic length of 2D system

$S$   $\equiv$  Cross-sectional area

The MT contribution to paraconductivity<sup>24</sup>, taking into account the shift in  $T_c$  due to pair breaking, may be expressed as

$$\sigma_{2D}^{MT} = [e^2 / 8\pi d (\epsilon - s)] \ln (\epsilon / s) \quad \dots (4)$$

$$\sigma_{1D}^{MT} = \sigma_{1D}^{AL} . 4 . (\epsilon / s) . [1 + (\epsilon / s)^{1/2}]^{-1} \quad \dots (5)$$

where  $s \equiv [T_c(\text{zero}) - T_c] / T_c$  is the reduced shift of  $T_c$  due to pair breaking.

Experimentally the excess conductivity may be determined<sup>25</sup> by first fitting the normal state resistivity  $\rho_N$  at high temperatures (e.g.  $1.5 T_c \leq T \leq 300K$ ) to linear form  $\rho_N = mT + C$ , and then extrapolating the straight line down to temperatures near  $T_c$ . The paraconductivity is usually taken to be  $P\sigma(T) = 1/D\rho(T)$  where  $D\rho(T)$  is the deficit resistivity at a temperature  $T$  defined as  $D\rho(T) = \rho(T) - \rho_N(T)$  where  $\rho(T)$  is the measured resistivity and  $\rho_N(T)$  the resistivity determined by extrapolating the linear  $\rho$  vs.  $T$  plot above  $T_c$ .

## 1.22 Abrupt Change in Specific Heat

The abrupt increase in the specific heat at  $T_c$  is a key signature of superconducting transition. [Fig. 1.2(b)]. The temperature dependence of specific heat in the superconducting state is very much different from that in the normal state and it

can give informations about electronic and vibrational excitations present in the superconductors both above and below  $T_c$ . The electronic specific heat above  $T_c$  is given by

$$C_{en} = \tau.T \quad \dots(1)$$

and that below  $T_c$  is described well by :

$$C_{es} = \tau.T_c.a \exp (-b.T_c/T) \quad \dots (2)$$

Where  $a$  and  $b$  are experimental constants having values of about 10 and 1.5, respectively. This exponential dependence on temperature suggests an average excitation energy of  $1.5 \text{ } kT_c$  in superconducting state, thus clearly indicating the presence of gap in superconductors.

In case of YBCO superconductors usually two jumps, one at  $T_{c1}$  ( $\approx 93^{\circ}K$ ) and the other at  $T_{c2}$  ( $\approx 89^{\circ}K$ ), are observed in specific heat vs. temperature plot<sup>26</sup>. One approach to analyse this type of data is to use a 3D Gaussian fluctuation around  $T_{c2}$  in the realm of G.L. Theory, ignoring the first jump at  $T_{c1}$  on the suspicion that either (a) a structural transition occurs or (b) there exists a more baroque possibility that two transition states order<sup>27</sup> at two different  $T_c$ 's. With this concept, the fluctuation specific heat is given by the following expression.

$$\Delta C = \frac{k}{4\pi c} \frac{1}{\epsilon_x(0).\epsilon_y(0)} \frac{1}{[\epsilon\{\epsilon+(2\epsilon_z(0)/c)^2\}]^{1/2}} \quad \dots (3)$$

For  $\epsilon \ll [2\xi_z(0)/c]^2$  also  $\bar{\xi}_{GL}(0) = [\xi_x(0)\xi_y(0)\xi_z(0)]^{1/3}$

Another approach is one in which both specific heat jumps are treated as intrinsic superconducting transitions<sup>26</sup> which order separately at two  $T_c$ 's without coexistence. This type of data may be analysed by using the standard Gaussian approximation<sup>26</sup>.

### 1.23 The Abrupt Change in Thermoelectric Power

If a superconductor in normal state is subjected to temperature gradient  $T$ , an electrical field  $\bar{E}$  will be developed, the coefficient  $sT/\bar{E}$  that characterizes the electromotive force resulting from the redistribution of carriers in the temperature gradient is defined as the thermoelectric power (TEP) or merely thermopower (TP). As shown in Fig. 1.2(c), the thermopower of a superconductor disappears at  $T_c$ . The temperature dependence of TEP for a typical superconductor may be expressed as<sup>27</sup>.

$$S_d = X_b T [1 + a \cdot \lambda \cdot \lambda_s(T)] \quad \dots (1)$$

where  $X_b \equiv S_b/T$  is the bare thermopower parameter

$a \equiv$  a Constant (equal to 1 in absence of velocity and relaxation time renormalization and Nelson Taylor effect

$\lambda \equiv$  The effective electron phonon enhancement at low temperatures

$\lambda_s(T)$   $\equiv$  Decay of thermopower enhancement with temperature

The magnitude of bare thermopower parameter (TPP),  $X_b$  is given by Mott. formula<sup>28</sup>

$$X_b = (\pi^2 k^2 / 3e) \cdot [d \ln \sigma(E) / dE] \quad \dots (2)$$

where  $\sigma \equiv$  Contribution towards electrical conductivity due to carriers of energy  $E$

The normalized temperature dependent enhancement of TEP,  $\lambda_s$  is usually expressed as<sup>27</sup>

$$\lambda_s(T) = \frac{\int_0^\infty dE E^{-1} \alpha^2 F(E) G_s(E/KT)}{\int_0^\infty dE E^{-1} \alpha^2 F(E)} \quad \dots (3)$$

where  $\alpha^2 F(E)$  is Eliashberg function

and  $G_s(E/KT)$  is Kaiser Universal Function.

It has been observed that superconducting bulk samples show a large dominant peak at the temperature at which the resistance drops most rapidly, followed by one or more subsidiary peaks in the region of foot of the resistive transition. It has been argued that the subsidiary peaks along with the foot indicate a series connection of regions with slightly different, but well defined  $T_c$ 's. The magnetic field dependence of position and height of the main peak suggests an interpretation in terms of fluctuation effects<sup>29</sup>, similar to specific heat and



resistivity<sup>30</sup>.

Although predicted to occur, such TEP fluctuations effect have, however, never been seen in the low temperature superconductors. This is because they typically have a zero temperature coherence length  $\xi(0) \gg 1000\text{\AA}$ , so that the temperature range over which one might expect to see such effects would be extremely small. In YBCO-super conductors, however,  $\xi(0)$  is thought to be  $\approx 1$  nm and the range over which one might observe 3D fluctuations could be several degree Kelvins.

#### 1.24 Perfect Diamagnetism in Superconductors-Abrupt Change in Magnetic Susceptibility :

Apart from the other peculiar properties of a superconductor, an important attribute of superconducting state is its ability to behave as a perfect diamagnet, able to expel other magnetic field, this effect is generally known as Meissner effect<sup>5</sup>. This effect exists upto a certain critical value of magnetic field usually referred to as critical field  $H_c$  beyond which the superconductor loses its perfect diamagnetism. The superconductors that remain diamagnetic only upto a rather low magnetic field  $H_c$  are called type I superconductors, these could not sustain large enough currents. On the other hand, the ones which can sustain superconductivity upto a much higher field  $H_{c2}$  are called type II superconductors. Between  $H_{c1}$  and  $H_{c2}$ , the superconductor is said to be in mixed state. The physical picture of this state is that of a bundle of filaments of normal state material generally called vortex lines in flux tubes arranged parallel to applied flux lines, and bathed in a sea of

superconducting material. The flux through a vortex line is quantized and has a value equal to integral multiples of  $\phi_0$  ( $=h/2e$ ), the basic quanta of flux.

In addition to the two parameters  $T_c$  and  $H_c$ , which are intrinsic characteristics of a superconductor; the superconducting state is also destroyed if the material carries a current density higher than a critical value  $J_c$ , called the critical current density. Thus the three parameters, viz., temperature, magnetic field and current density, determine together whether a material would remain superconducting or not. The superconducting state thrives below and vanishes above a 3D critical surface unique to each superconductor. The projection of this surface on H-T plane gives the temperature dependence of critical field. Fig. 1.2(g) shows such a projection for a typical superconductor, this is very often called a phase diagram as it separates the two, non-superconducting and superconducting phases. From here one can readily see that

$$H_c(T) = H_c(0) [1 - (T/T_c)^2] \quad \dots (1)$$

where  $H_c(0)$  is the critical field required to destroy the superconductivity at absolute zero.

Fig. 1.2 (d) shows a typical susceptibility vs. temperature plot for a superconductor. It is easy to see that the susceptibility has a approximately linear dependence on temperature in high temperature regime. Moreover, one can readily perceive a diamagnetic deviation from linearity at low temperatures. This diamagnetism is reasonably attributed to

superconducting fluctuation effect because they grow progressively as the temperature approaches  $T_c$ . Prange<sup>31</sup> showed that magnetization  $M'$  due to these fluctuation effects may be written as :

$$M' / H^{1/2} T = f(x) \quad \dots (2)$$

where  $f$  is a universal function of  $x [= (dH/dT) \cdot \{T - T_c(\text{zero})\} / H]$

This fluctuation magnetization is small, we may safely neglect the difference between  $B$  and  $H$  in calculating zero field susceptibility. Schmid<sup>32</sup> found the following expression for zero field susceptibility :

$$\chi' = \pi \cdot kT \cdot \xi(T) / 6 \cdot \phi_0^2 \approx 10^{-7} \epsilon^{-1/2} \quad \dots (3)$$

where  $\phi_0 \equiv hc/e$  flux quanta ( $= 2.07 \times 10^{-7} \text{ G cm}^2$ )

$\epsilon \equiv$  Reduced temperature  $(T - T_c) / T_c$

This susceptibility is same of magnitude as Landau diamagnetism of normal metals apart from the temperature dependent enhancement factor  $\epsilon^{-1/2}$  and is many orders of magnitude smaller than the full diamagnetic susceptibility in Meissner state [ $\chi = -1/4 \pi$ ]

### 1.25 Characteristic Change in Microwave Absorption

The electromagnetic response of superconductors at high frequencies provides unique informations regarding the nature and

potential for device application at these frequencies. it is well known that superconductors absorb microwaves when  $h\nu \geq 2\Delta$ ,  $2\Delta$  being the superconducting energy gap and  $\nu$  the frequency of microwave. However, the absorption can not occur when  $h\nu \ll 2\Delta$ . The microwave absorption has been shown to be sensitive to magnetic field and hence to flux penetration in high  $T_c$  oxide superconductors<sup>33</sup>. Fig. 1.2(e) shows a typical microwave absorption vs. magnetic field plot for a superconductor at a temperature slightly below  $T_c$ . At low field side a pronounced bend is observed which marks the position of  $H_{c1}$  and corresponds to the flux penetration to individual crystallites. After this bend the absorption  $I(H)$  is found to be nearly proportional to  $H$ .  $I(H)$  may be expressed as

$$I(H) = A(T).H + C(T)$$

The first term  $A(T).H$  represents the contribution similar to type II superconductors which is believed to arise from superconducting grains, while  $C(T)$  is due to the decoupling of weak Josephson links due to magnetic field, microwave current and/or thermal fluctuations<sup>34</sup>.

The zero-field microwave absorption in High  $T_c$  superconductors has also been the subject of considerable study Fig. 1.2(f) shows a typical zero field microwave absorption as a function of temperature. This absorption in superconducting pellet samples arises from the intergranular boundary regions, other inhomogeneities and defects<sup>35</sup>.

### 1.3 Current Theoretical Status in High Tc Superconductivity

Since the discovery of superconductivity, a number of theoretical models have been proposed to explain the phenomenon. For classical low temperature superconductors theories, like London theory<sup>6</sup>, non local generalization of London theory i.e. Pippard model<sup>8</sup>, Ginzburg-Landau theory and Abrikosov's reversal<sup>7</sup> and well known BCS theory<sup>9</sup> were proposed. These theories especially the BCS theory, were found quite satisfactory for classical superconductors, but have failed completely to explain the observed properties in newly discovered high Tc oxide superconductors.

The oxide superconductors have been subjected to a plenty of theoretical work. Various theories have been proposed. Almost all viable theories propose a form of carrier pairing as being responsible for superconductivity. There are ample experimental evidences for the pairing of carriers in superconductors e.g. :

- (1) the Shapiro steps in Josephson tunnel junctions biased with ac and dc voltages have a spacing  $\Delta V = 2 e/h\nu$  , clearly indicating an effective charge  $2e$ .
- (2) the flux quantum in a high Tc superconducting ring has been found out to be  $\phi_0 = h/2e$ .
- (3) experimental verification of mixed state in type II superconductors and flux quantization through the vortex lines.
- (4) the exponential dependence of specific heat on temperature, which predicts an average excitation energy of  $1.5KT_c$ . i.e., there exists a gap in the high temperature

superconductors which has been found twice that of thermal gap. This may be understood only if carriers occur as pairs.

In a conventional BCS type superconductor  $\sim 10^6$  electrons are there within the average distance between mates of a single pair<sup>36</sup>. So that the pairs do not truly obey the Bose-Einstein statistics, but the Pauli principle plays an important role. Thus it puts a restriction on Bose condensation of pairs. This suggests a classification of theories into two groups.

### 1.31 BCS Type Theories

The BCS theory predicts the  $T_c$  very low (maximum  $\sim 40K$ ). So important issue is to understand as to why the  $T_c$  of CuO superconductors is so high. In weak coupling limit  $T_c$  can be expressed as :

$$kT_c = 1.14\hbar\omega_c \exp [-1/N(0)V] \quad \dots (1)$$

where  $\hbar\omega_c$  is the cut of energy comparable to the maximum energy of excitations which mediate the pairing within the BCS framework. There are three ways to increase  $T_c$ , viz., by increasing (i)  $N(0)$ , the density of states at Fermi surface, (ii) The effective electron-electron attraction  $V$  and (iii)  $\omega_c$ ; the cut of frequency.

According to earlier theories proposed by Ginsburg<sup>37</sup> and Allender<sup>12</sup>, an attractive interaction between carriers can be mediated by the exchange of virtual electron hole pairs, the so called excitonic mechanism for superconductivity. In order for

this mechanism, to work, two distinct types of carriers are required; conducting carriers in a metallic region (chain or plane); which pair to form the superconducting condensate, and polarizable electrons in adjacent region (side chain or plane) which interact with the metallic carriers to mediate the pairing process. It is possible that the polarizable, non conducting electrons in the BaO planes or the carriers in CuO chains may mediate a pairing between the conducting carriers in CuO planes in the YBCO compound. On the other hand, according to theory of 'Charge transfer excitation exchange' proposed by Varma and coworkers<sup>13,38</sup>, the virtual electronic polarization occurs through the transfer between copper and oxygen sites within a CuO plane. In this picture the same carriers which mediate the pairing process also participate in forming the superconducting condensate.

The exciton mechanism<sup>39</sup> is predicted to yield a significantly higher  $T_c$  than the phonon mechanism because the cut off energy  $\hbar\omega_c$  is expected to be comparable to the electronic excitation energies, which are generally much higher than typical Debye energies. In this excitonic system the interaction is mediated by the movement of electrons rather than by the much heavier ions of a phonon superconductor. The transition temperature for an excitonic superconductor would thus be scaled up from that of conventional superconductors by a factor of the order of  $(M_{ion}/m_e)^{1/2}$ , if all other parameters were kept constant. Similar arguments hold for theories proposing the exchange of plasmons<sup>13,39</sup> or virtual magnetic excitations, such as antiferromagnetic spin fluctuations<sup>40</sup>. Again, the higher

energies of the relevant virtual excitations increase the energy range over which the electron electron interaction is attractive, leading to a higher fraction of paired carriers and thus a higher  $T_c$ .

One can easily infer from the above discussion that this class of theories assume that the pairs are formed at  $T_c$  only and that it is the pairing between carriers via certain virtual excitations only which is responsible for superconductivity.

### 1.32 Bose Condensation Type Theories

These theories assume that pairs already exist above  $T_c$ . The unpaired carriers follow Fermi-Dirac Statistics, but as soon as pairing takes place the statistics of the particles change to Bose-Einstein wherein the distribution function is given by

$$f_{BE} = [\exp(\alpha + \beta E) - 1]^{-1} \quad \dots(1)$$

where  $\beta = 1/kT$  and  $\alpha$  is given by the equation

$$e^{-\alpha} = n h^3 (2n_m^* kT)^{-3/2}; \text{ with } n \text{ as concentration of the integral spin particles of effective mass } m^*.$$

Here more than one particles can occupy the same state contrary to Fermi-Dirac (FD) statistics. The maximum number of particles  $n'$  occupying states above ground state in BE statistics is given by

$$n' = n (T/T_0)^{3/2}; \text{ when } T < T_0 \quad \dots(2)$$



where  $n$  is the concentration of particles and  $T_0$  is the temperature when  $\alpha$  of Equation (1) is zero. Hence, the number of remaining particles  $n_0$  is given by

$$n_0 = n - n' = n [1 - (T/T_0)^{3/2}] \quad \dots(3)$$

As the temperature is lowered, beginning at  $T = T_0$  the particles fall rapidly into ground state. This is some sort of condensation generally called Bose condensation.

One of the leading theories for high temperature superconductors of this class is the Resonating valence bond (RVB) Model<sup>41,42</sup> proposed by Anderson and coworkers. According to this model, the pairing mechanism is magnetic in origin and not of conventional BCS type. The basic idea of RVB theory is that strong electron-electron correlations result in a separation of charge degree of freedom from the spin degree of freedom. The starting point of RVB theory is a 2D Hubbard model at half filling with strong on site. Coulomb repulsion  $U$  and an attractive intersite hopping energy  $T$ , without oxygen doping (i.e.  $x = 0$ ), the ground state of the above model is expected to be a long range antiferromagnetic (AF) state, but Anderson argued that the frustration might favour a RVB state over an AF ground state.

At low doping ( $x \neq 0$ ) and temperature, the quasi-particle excitations are believed to be holons (i.e. charge carrying spinless particles) and spinons (i.e. spin  $(-1/2)$  chargeless particles). Superconductivity is due to formation of a condensate consisting of holon-pairs. Since BE condensation is

not possible in a strictly 2D system, the inter-planer couplings are important in giving rise to superconductivity.

Another theory that has been proposed is the Bipolaron mechanism<sup>43</sup>. Here the high  $T_c$  superconductors are considered to be as doped semiconductors<sup>44</sup> where the conductivity is due to doping or self-doping. This produces mixed valence-conditions for the metal ions, leading to the formation of small-polarons, i.e the combination of the metal atom with its extra charge plus its deformed oxygen coordination. The mobility of these small polarons is ensured through the mixed valence charge transfer mechanism. They may be viewed as dilute gas of charged particles in a lattice moving in the random fluctuating potential due to impurities. It is further argued that under special conditions these small polarons, may combine to form small bipolarons and the possible binding mechanism may be the carrier lattice exchange<sup>45</sup>. The bipolarons act like a weakly interacting Bose gas capable of condensing into its ground state at relatively elevated temperatures and hence becoming superconducting.

There are numerous other theories on high  $T_c$  superconductivity whose description is beyond the scope of the present Chapter. However, a summary of various proposed pairing mechanisms is presented in Table 1.4 indicating their classification according to mode of pairing.

#### 1.4 Crystal Structure of YBCO High Temperature Superconductors

The superconducting properties have direct relation with the structural aspects of the material. To examine this, let us

consider the crystal structure and its consequences for the YBCO superconductor, a well known high temperature superconductor which has been subjected to a large number of experimental and theoretical investigations and represents a typical example of high  $T_c$  superconductors.

The high temperature superconducting phase in YBCO system has an orthorhombic Pmmm structure with a single formula unit  $\text{YBa}_2\text{Cu}_3\text{O}_7$  per primitive cell. It can be viewed as a defect perovskite lattice  $(\text{Y-Ba})_3\text{Cu}_3\text{O}_{9-x}$ , based on three Cu centered perovskite cubes (hence the name triple perovskite structure) with both O vacancy and Y-Ba ordering along the c-axis. Of the two O vacancies (corresponding to  $x = 2$ ), one occurs in every third Cu-O plane along the a-axis (say) at the site  $(1/2, 0, 0)$ , resulting in the orthorhombic symmetry, see Fig. 1.3(a).

The structure of orthorhombic YBCO is interesting, as it has corner linked  $\text{CuO}_4$  planar group connected not only to sheets in the ab plane but also as chains parallel to b axis. Of the two sets of Cu atoms, one is surrounded by 5-oxygens giving rise to a square pyramidal coordination for Cu and thus forming puckered  $\text{CuO}_2$  sheets. In the other set, however, the Cu atoms are surrounded by 4-oxygens, here the oxygen atoms form near rectangles connected by vertices and resulting in chains O-Cu-O along the b axis. YBCO structure may be viewed as a stacking of two sheets of  $\text{CuO}_2$  type bound together by an array of parallel O-Cu-O linear sticks. This obviously brings the coordination of Cu in  $\text{CuO}_2$  sheets to five and forms a sandwich containing 2- $\text{CuO}_2$  sheets and the array of parallel O-Cu-O sticks. The Ba cations fit into cavities within this sandwich The Y cations are found

between sandwiches and they bind the sandwiches together to form a 3D structure from the 2D sandwiches.

#### 1.41 Role of Oxygen

It has been pointed out that oxygen content seriously affects the superconducting properties of YBCO-compounds<sup>46</sup>. The superconducting  $\text{YBa}_2\text{Cu}_3\text{O}_{7-\delta}$  becomes non-superconducting at  $\delta = 1$  and the O-Cu-O chains are missing as shown in Fig. 1.3(b). This system may be described by the composition  $\text{YBa}_2\text{Cu}_3\text{O}_6$  having tetragonal symmetry. The missing of chain i.e. removal of an O ion from chain modify the oxygen occupancy, now oxygen occupy only  $2/3$  of the perovskite anion sites and are ordered in such a manner that the one third of the Cu atoms is two fold coordinated while two third is five fold coordinated<sup>47</sup>. In the range  $0.6 \leq \delta \leq 1.0$  the YBCO exists in the tetragonal form and has very few oxygens in the O-Cu-O chains, this gives rise to considerable oxygen disorder and hence to distorted  $\text{CuO}_6$  octahedra as shown in Fig. 1.3(c). Oxygen non-stoichiometry in YBCO system has, therefore, to be understood in terms of both disorder and structural distortion.

The variation of superconducting transition temperature  $T_c$  of orthorhombic  $\text{YBa}_2\text{Cu}_3\text{O}_{7-\delta}$ , with  $\delta$  in the range 0-0.5, is most interesting. The  $T_c$  is nearly constant around 90K at low  $\delta$  (0.0-0.2) and then drops to lower value ( $\sim 50\text{K}$ ) above  $\delta = .2$  showing a plateau like behaviour. It is believed that this 50K plateau is essentially a characteristic of superconductivity due to  $\text{CuO}_2$  sheets, as for these values of  $\delta$ ; the O-Cu-O chains are rather depleted of oxygen<sup>48</sup>. Thus this dependence may therefore be

taken to signify a transition from chain type superconductivity to sheet type superconductivity in orthorhombic YBCO brought about by the change in oxygen stoichiometry.

#### 1.42 Crucial Role of Copper in Superconductivity

Since the discovery of superconductivity in oxide ceramics, the role copper and its oxidation state have widely been debated. Using charge balancing for one formula unit some amount of Cu is expected to be in  $3+$  state. Photo-electron spectroscopy has been used by several workers primarily in the  $\text{Cu}(2\text{P}_{3/2})$  region, for distinguishing contributions from the various oxidation states<sup>49,50</sup>. The comparative XPS study has also revealed<sup>51,52</sup> a number of facts about the oxidation state of copper in YBCO. The 2P-Photo-emission final state for  $\text{CuO}$  and related compounds with formal  $\text{Cu}^{2+}$  is not found to be simple as they are accompanied by strong satellites, corresponding to the configuration  $(\text{P}^5\text{d}^9)$ , alongwith the main line, corresponding to configuration  $(\text{P}^5\text{d}^{10}\text{L})$ , L being the Ligand-hole. However the structure and position of the satellite is sensitive to the chemical surrounding of the copper ion and depends strongly on the electro negativity of the ligand<sup>53</sup>. The satellite intensity is strongest and satellite main peak separation largest when the ligands are of high electronegativity. It has been shown<sup>51</sup> by XPS studies that energy separation  $\text{d}^9\text{-d}^{10}$  is larger for tetragonal non superconducting YBCO than the orthorhombic phase by an amount of  $\sim 0.5\text{eV}$ , reflecting the fact that electronegativity of the ligand is more for superconducting phase than for non-superconducting phase. With respect to the Cu sites

this would mean a localization of 3d-electrons and a tendency towards  $\text{Cu}^{2+} \rightarrow \text{Cu}^{1+}$  transition. Such an effect has indeed been noticed in the valency bond photo-emission studies<sup>54</sup>. The Fourier summation technique as applied to X-ray diffraction data<sup>55</sup> of YBCO revealed that the estimated atomic charges belonging to Cu(I) and Cu(II) atoms are +0.988e and +1.787e, suggesting that univalent  $d^{10}$  and divalent  $d^9$  ionic states are present. The atomic charges quoted above coincide with the electron distribution around Cu atoms observed from Difference Fourier analysis<sup>56</sup>. It has been envisaged that  $\text{Cu}^{1+}$  plays a vital role in superconductivity as it forms singlet-pair, generally called peroxiton, composed of  $\text{O}^-\text{Cu}^+\text{O}^-$  type species. Chakravorty et. al.<sup>32</sup> pointed out that this forms a RVB state which as a result of Bose-condensation gives the super conductivity.

There are some reports wherein the  $\text{Cu}^{3+}$  ions are said to be found<sup>57</sup> in both superconducting and nonsuperconducting YBCO. The later determinations have however, shown this to be incorrect. In absence of  $\text{Cu}^{3+}$ , the only possibility is that the holes reside on the oxygen orbitals<sup>58</sup>, the role of which has already been discussed in the previous paragraph.

### 1.5 Substitutional Studies in YBCO superconductors

If new superconducting materials with improved  $T_c$  and other superconducting properties are to be discovered, we have to first determine the mechanism of the superconductivity, which of course, has not been well understood so far. An immense amount of work has been directed towards this goal, one important

approach for this is the addition of other ions as a substitution for one or more ions in the superconducting materials. These substitutional studies are performed to meet the following specific goals.

- (a) To reveal the acceptability of the impurity and its level at the specific position in the structure and the crystal chemical consequences e.g. single or multiphase system.
- (b) To reveal the effects on the superconducting properties of new single phase or multiphase materials.
- (c) To reveal other important effects such as
  - (i) The chemical stability in the ambient
  - (ii) Physical properties e.g. density, mechanical strength
  - (iii) Reliability e.g. electric and magnetic properties with time i.e. the aging effects.
- (d) To optimize the processibility of the superconducting ceramics
- (e) To provide important clues towards compatibility of the superconducting materials with other electronic materials to be incorporated in a variety of devices.
- (f) To elucidate the contributions and effects of various cations' and anions' sites on the electronic structure in superconductors and thus to expedite the mechanism of superconductivity.
- (g) To understand the role of constituent ions in a superconductor and hence to get the idea about the essential ingredients for superconductivity.

Based on the extensive studies of additives to the YBCO superconductor, it is clear that a very large number of ions can be substituted for Y, Ba, Cu and O. Generally two types of substitutions are possible.

- (i) Isovalent substitutions : In this case host ion is replaced by an ion of the same valency. This type of substitutions are possible at all anionic and cationic sites in YBCO superconductors.
- (ii) Aliovalent substitutions : In this case the substituting ion is of a different valency than the host ion. This type of substitution is possible at cationic sites only in YBCO superconductors.

Table 1.6 gives the various cation/anion substitutions reported in literature on YBCO superconductor. In general, the substitution at Cu and O sites were found to effect the superconducting properties drastically. These two shall be considered separately.

#### 1.51 Substitutions at Cu Sites :

As evident from structural aspects of YBCO, the  $[\text{Cu}(1)-\text{O}]_m$  type quasi linear chains (1D) stack with the 2D  $[\text{Cu}(11)-\text{O}]_n$  sheets. This arrangement contains two equivalent Cu sites. One is between two Ba ion layers and forms the chain, while the other is with pyramidal coordination of oxygen in  $[\text{Cu}(II)-\text{O}]_n$  sheets. The fact that which part of the chain or sheet is most responsible for high  $T_c$  superconductivity in YBCO is an



interesting point for studying the new superconducting mechanism. As an approach, substitutions of other elements at the Cu-sites can be considered. When the substitute has a character of site preference for Cu(1) or Cu(2), we can check the responsibility of each site to superconductivity by observing changes in  $T_c$ . Consider, for example, the substitutions of Ni and Zn. In this case, the substitution mainly occurs at planar Cu(II) sites where as for Co, Fe and Al it occurs preferentially<sup>59</sup> on linear chain sites Cu(I). So the important question is which Cu-site should be occupied by a substituent. In a unit cell of  $YBa_2Cu_3O_{7-\delta}$  copper occupies two Cu (II) sites and one Cu(I) site. Kasperczyk et al<sup>60</sup> considered this problem in case of transition metal substitutions and pointed out that the crystal field stabilization energy for each transition metal ion  $E_{CF}$  depends on the number of 3d electrons and energy splitting parameter, the later being different for two sites of copper. Within the Boltzmann distribution, the probability of occupying a Cu-site by transitional ion at sintering temperature  $T_s$  is given by

$$P_o = 2 \exp [-E_{CF}^o/kT_s] / [2 \exp (-E_{CF}^o/kT_c) + \exp (-E_{CF}^t/kT_s)] \quad \dots (1)$$

$$P_t = \exp [-E_{CF}^t/kT_c] / [\exp (-E_{CF}^t/kT_s) + 2 \exp (-E_{CF}^o/kT_s)] \quad \dots (2)$$

Here o-denotes octahedral and t, tetrahedral sites. Thus an average number of atoms of metal M substituted, is equal to  $3XP_t$ , per unit cell in 1D structure of  $YBa_2(Cu_{1-x}M_x)_3O_{7-\delta}$  system.

The values of  $(E_{CF}^o - E_{CF}^t)$  for Ti, Cr, Mn and Ni are large<sup>61</sup> which give  $P_o \gg P_t$ , i.e., these atoms occupy mostly Cu(II) positions and influence the superconducting coupling to small extent. Fe and Co have smaller differences in stabilization energies and therefore occupy Cu(I) site in 1D ribbon decreasing  $T_c$  significantly. A special case is of  $Zn^{2+}$  for which  $E_{CF}^o - E_{CF}^t = 0$ , because of its  $d^{10}$  configuration it may occupy both sites.

### 1.52 Substitution at Oxygen Site

The oxygen content is a major controlling parameter for the superconducting properties. Introduction of vacancies at oxygen sites is known to be associated with a huge reduction in  $T_c$  of YBCO superconductors<sup>62</sup>. However this change is associated with complicating structural modifications, and it is of interest to investigate dopants that are directed at the sensitive oxygen site, but that leave the structure unchanged. Table 1.6 lists some of the possible substitutions at oxygen sites. Except a few reports almost all substitutions leave the compound with a decreased  $T_c$ , however properties like  $J_c$  are drastically improved. The reports<sup>63,64</sup> of higher  $T_c$  in sulphur and fluorine substituted YBCO were found not to be reproducible<sup>65,66</sup>.

A carefully controlled absorption of gas in YBCO has, however, been found to improve the superconducting properties. The effect has now been observed with a number of gases such as Nitrogen<sup>67,68</sup>, Helium<sup>69</sup>, Argon<sup>68</sup> etc. In case of hydrogen however, a decrease in  $T_c$  is observed<sup>70</sup>. The mechanism by which this drastic change occurs is not clear so far but it is believed that it may be associated with a catalytic absorption of gas into

the relatively open structure of YBCO lattice.

## 1.6 Statement of the Problem

With a view to improve the superconducting properties and also to gain an insight in the mechanism of superconductivity, a large number of substituted YBCO systems have been, and are still being, investigated. Many dopants in place of Y and Ba in  $\text{YBa}_2\text{Cu}_3\text{O}_{7-\delta}$  have been tried but they have failed to increase the  $T_c$ . These studies have further strengthened the view that CuO is the most critical ingredient for the high  $T_c$  superconductors, and hence its replacement by a suitable material should bring about desirable changes in the YBCO superconductors.

The properties of CuO, especially its high dielectric constant, modest resistivity, multivalence state, etc., should be considered while looking for its equivalent substituents. Silver oxide(s) should have been a natural choice for CuO but as both silver oxides are unstable at high temperatures; AgO decomposes at  $120^\circ\text{C}$  and  $\text{Ag}_2\text{O}$  at  $230^\circ\text{C}$ , however,  $\text{Ag}_2\text{S}$  is stable and hence is a good substituent for CuO. The other materials that may be considered in place of CuO are lead salts. In the present work PbS was chosen in view of the following similarities.

- (i) Both CuO and PbS have relatively high and nearly same value of dielectric constant, 18.1 (at  $10^8$  Hz) and 17.9 (at  $10^6$  Hz) respectively, at  $15^\circ\text{C}$ .
- (ii) Both Cu and Pb based oxides show superconductivity (e.g.  $\text{Y}_1\text{Ba}_2\text{Cu}_3\text{O}_{7-\delta}$  and  $\text{BaPbO}_3$ ). Also the sulfides and oxide (binary or ternary) show superconductivity, and hence it is reasonable to think of doping Pb at Cu-site and S at O-

site, i.e., PbS in place of CuO.

(iii) Both Pb and Cu are transition elements, while S and O are in the same group (VI).

This thesis reports the synthesis of pure and PbS-doped YBCO high  $T_c$  superconductors, and their structural characterization by means of XRD, SEM-EDX, etc. and electrical resistivity measurements.

Table 1.1

Some representative superconducting elements

Element	Tc (K)	Element	Tc (K)	Element	Tc (K)
Aluminium	1.75	Thallium	2.38	Niobium	9.25
Indium	3.408	Tin	3.722	Protactinium	1.4
Lead	7.196	Tungsten	0.0154	Technetium	7.8
Molybdenum	0.915	Zinc	0.85	Thorium	1.38
Osmium	0.66	Cadmium	0.517	Titanium	0.4
Rhenium	1.697	Iridium	0.113	Vanadium	5.40
Tantalum	4.47	Mercury-	4.154	Zirconium	0.61

Table 1.2

Superconducting transition temperatures and critical fields for some representative alloys and intermetallics.

	T <sub>c</sub> (K)	H <sub>c</sub> (K Gauss)
<b>Alloy</b>		
Pb-Sb	6.6	-
Nb-Ti	12.0	180
Nb-Zr	6.0	180
Mo-Re	11.0	20
Mo-Tc	14.0	20
<b>Compounds</b>		
A-15, Nb <sub>3</sub> Ge	23.3	250
C-15 (HZr)V <sub>2</sub>	10.15	250
Nb <sub>3</sub> Sn	18.0	-
Nb <sub>3</sub> Al	18.0	-
V <sub>3</sub> Si	17.1	-
V <sub>3</sub> Ga	16.8	-

Table 1.3

## High temperature oxide superconductors

System	T <sub>c</sub> (K)	Remarks
<u>La-System</u>		
(i) $(\text{La}_{1-x}\text{M}_x)_2\text{CuO}_4$ x=0.2 M=Ba, Sr, Ca	25-40	K <sub>2</sub> NiF <sub>4</sub> Structure
(ii) $\text{La}_1\text{Ba}_2\text{Cu}_3\text{O}_7$	90	-
(iii) $\text{La}_{2-x}\text{Na}_x\text{CuO}_4$	40	K does not work
(iv) $(\text{Bi}_{1-x}\text{La}_x)\text{SrCuO}$	40	-
(v) $\text{La}_{2-x}\text{CuO}_{4-y}$	40, 90	-
(vi) $\text{La}_2\text{Ba}_3\text{LuCu}_6\text{O}_y$	50	-
<u>Y System</u>		
(i) $\text{Y}_1\text{Ba}_2\text{Cu}_3\text{O}_{7-y}$	90	Y can be replaced by Lanthenide ions (except Ce, Pr, Tb)
(ii) $\text{Y}_2\text{Ba}_4\text{Cu}_8\text{O}_{20-x}$	80	-
<u>Bi System</u>		
(i) $\text{Bi}_2\text{Sr}_2\text{Cu}_1\text{O}_y$	7, 20	semiconductor, single CuO <sub>2</sub> layer
(ii) $\text{Bi}_2\text{Sr}_2\text{Ca}_1\text{Cu}_2\text{O}_y$	85	double Cu-O <sub>2</sub> layer
(iii) $\text{Bi}_2\text{Sr}_2\text{Ca}_2\text{Cu}_3\text{O}_y$	110K	triple CuO <sub>2</sub> layer
(iv) $\text{Bi}_2\text{Sr}_2\text{Ca}_3\text{Cu}_4\text{O}_y$	90	-

Contd/-

Tl-System

(i)	$\text{Tl}_2\text{Ba}_2\text{Cu}_1\text{O}_y$	20.80	Single $\text{CuO}_2$ layer
(ii)	$\text{Tl}_2\text{Ba}_2\text{Ca}_1\text{Cu}_2\text{O}_y$	105	double $\text{CuO}_2$ layer
(iii)	$\text{Tl}_2\text{Ba}_2\text{Ca}_2\text{Cu}_3\text{O}_y$	125	triple $\text{Cu-O}_2$ layer
(iv)	$\text{Tl}_1\text{Ba}_2\text{CuO}_y$	0	Single Tl-O
(v)	$\text{Tl}_1\text{Ba}_2\text{Ca}_1\text{Cu}_2\text{O}_y$	80	..
(vi)	$\text{Tl}_1\text{Ba}_2\text{Ca}_3\text{Cu}_3\text{O}_y$	110	..
(vii)	$\text{Tl}_1\text{Ba}_2\text{Ca}_3\text{Cu}_4\text{O}_y$	120	..

---

Other systems

(i)	$\text{Nd}_{1.6}\text{Sr}_{0.2}\text{Ce}_{0.2}\text{CuO}_4$	27	$\text{Nd}_2\text{CuO}_4(?)$ or not
(ii)	$(\text{Tl}_{0.75}\text{Bi}_{0.25})_{1.33}$	7.5	-
	$(\text{Sr}_{0.5}\text{Ca}_{0.5})_{2.7}\text{CuO}$		

---



Table 1.4

Some of the pairing mechanisms in high temperature superconductors

Virtual excitations	Type of Pairing	
	BCS pairing	Base Condensation
Phonons	Conventional	Bipolaron formation
Magnetic correlation	Exchange of anti-ferromagnetic (AFM) spin-fluctuations	Resonating valency band (RVB) or spin bipolaron formation and Bose condensation or boson pair formation followed by condensation
Electronic polarization Resonance	Excitons/Electron-hole pairs/charge transfer excitations/ soft plasmons or plasmons	-

Table 1.5

Comparison of salient features of superconducting cuprates

Feature	La-system	Y-system	Bi-system	Tl-system
T <sub>c</sub>	30-40	90K	80-110K	90-125K
Dimensionality	2	2	2	2
Crystal Structure	Orthorhombic	Orthorhombic*	orthorhombic	orthorhombic (tetragonal) <sup>+</sup>
Space group	D <sub>2h</sub> <sup>18</sup> Abma, Bmba or Cmca	D <sub>2h</sub> <sup>1</sup> (Pmmm)	-	-
Cu-coordination	square planar	square planar	square planar	square planar
Oxidation state of Cu as found	1+/2+	1+/2+	1+/2+	1+/2+

\* Some high T<sub>c</sub> tetragonal 123 compounds have been made

+ Although tetragonal structures have generally been assigned, crystal with orthorhombic structure have been found by electron diffraction

Table 1.6

## Cationic/ Anionic Substitutions in YBCO High Temperature Super Conductors

Cationic/ anionic site	Substituting ion	Reference(s)	Remarks
Y-site	Lanthanides $\text{Ln}^{3+}(1)$	71-73	c, negligible effect on $T_c$
	Pr(1)	74	p, $T_c$ decreases drastically
	La(1)	75	p, $T_c$ decreases
	Ca(a)	76,77	p, $T_c$ decrease slightly Cu remains as $\text{Cu}^{2+}$
	Bi(a)	78	p, $T_c$ decreases slightly, normal State resistivity increases
	Fe(a)	79	p, $T_c$ decreases, Fe ion ordering
Ba-site	Rare earths(a)	80	p, $T_c$ decreases
	Mg(1)	81	p, $T_c$ decreases drastically
	Alkaline earths(a)	82,87	p, $T_c$ decreases. very slightly. Sintering temp. decreases.
	La(a)	83,84	p, First $T_c$ increases then decreases with doping concentration.
	Sr(1)	85,86	p, $T_c$ decreases
	Pb(1)	88	p, superconducting properties like $J_c$ are improved, but $T_c$ decreases.
	36 elements including all types	115	p, different effects are observed for different elements.

contd/-

Cu-sites	Transitional metals (i)	89 - 91, 103,110 116	p, Tc decreases rapidly
	nobel metals(a)	91 - 93, 105,110	p,Tc remains almost same in low conc. range of substitution
	W(a)/Nb	94	p,Tc almost unchanged 3-fold increase in Jc
	Pb(i)	95 - 97 110	p,Tc decreases rapidly while Jc increases by 1-2 orders of magnitude
	Ga(a)	98,99	p,Tc fall with increasing doping
	Nd(a)	100	p,Tc decreases rapidly
	V(a)	101	p,No effect on Tc transition becomes broader.
	Mn(i)	102	p, Normal state resistivity increases, superconducting volums fraction decreases
	Ti(i)	104	p,Tc increases upto 95K.
	Si(i)	109	p,Tc increase with conc. first and then decreases
	Sn(i)/Cd(i)	110,114	p, Tc decreases

---

Contd/-

O-site	VI p element(i) 106,63,66 (Chalcogens.)	p, No confirmed trend in Tc change, Jc however increases 3-4 times.
	VII a element(a) 88,107, (halogens) 64-66	p, Tc reported to increase
	N <sub>2</sub> (absorption) 67,68	Tc increases (Tc max = 141K)
	He (absorption) 69	Tc increases
	Ar (absorption) 68	Tc increases. The effect is very efficient
	H <sub>2</sub> (absorption) 70,108	Tc decreases.

---

Note : i and a stand for isovalent and aliovalent respectively,  
p and c stand for partial and complete substitution.

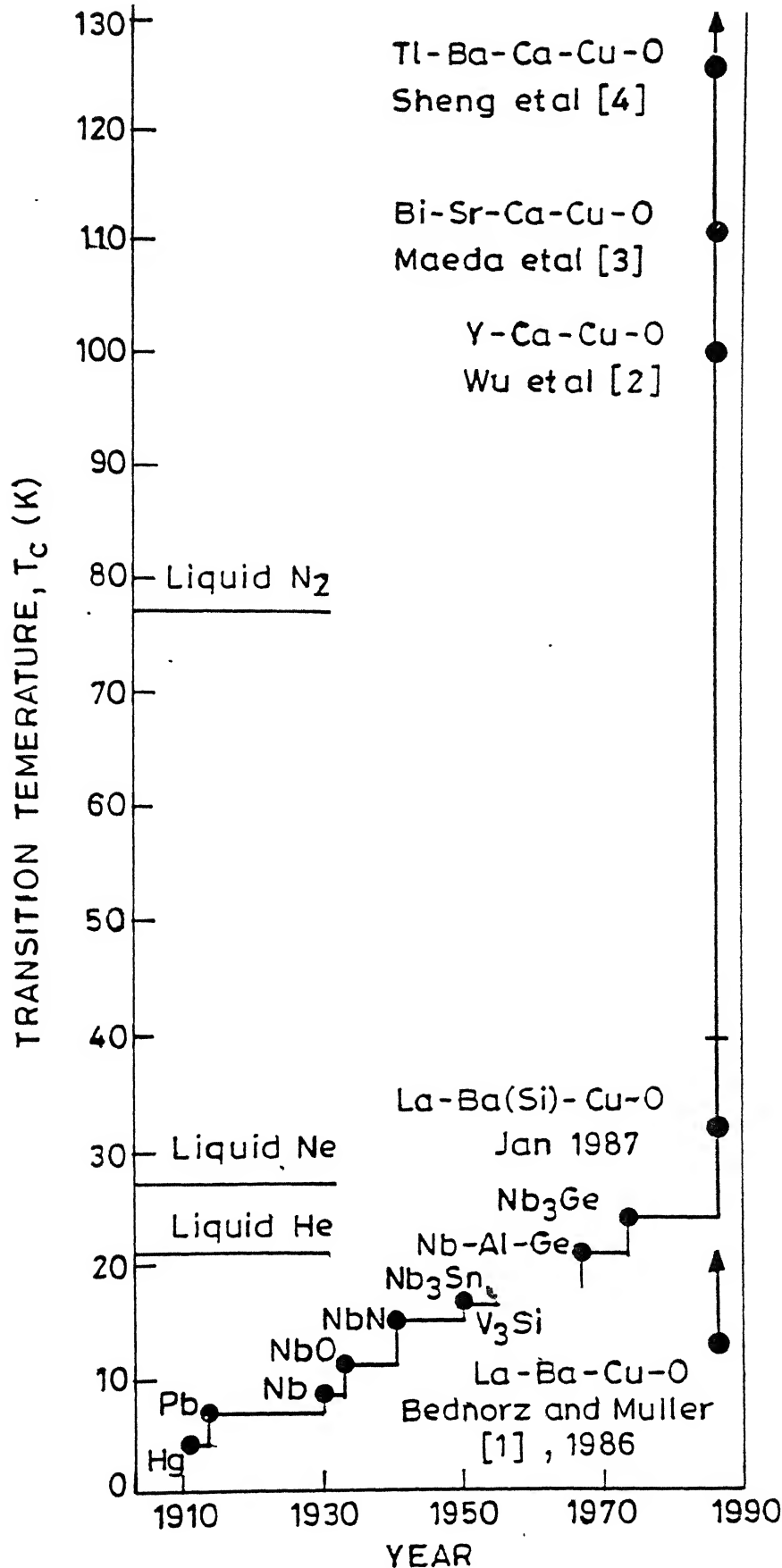


FIG. 1.1 CHRONOLOGY OF EVENTS AND HALLMARK DEVELOPMENTS IN SUPERCONDUCTIVITY RESEARCH.

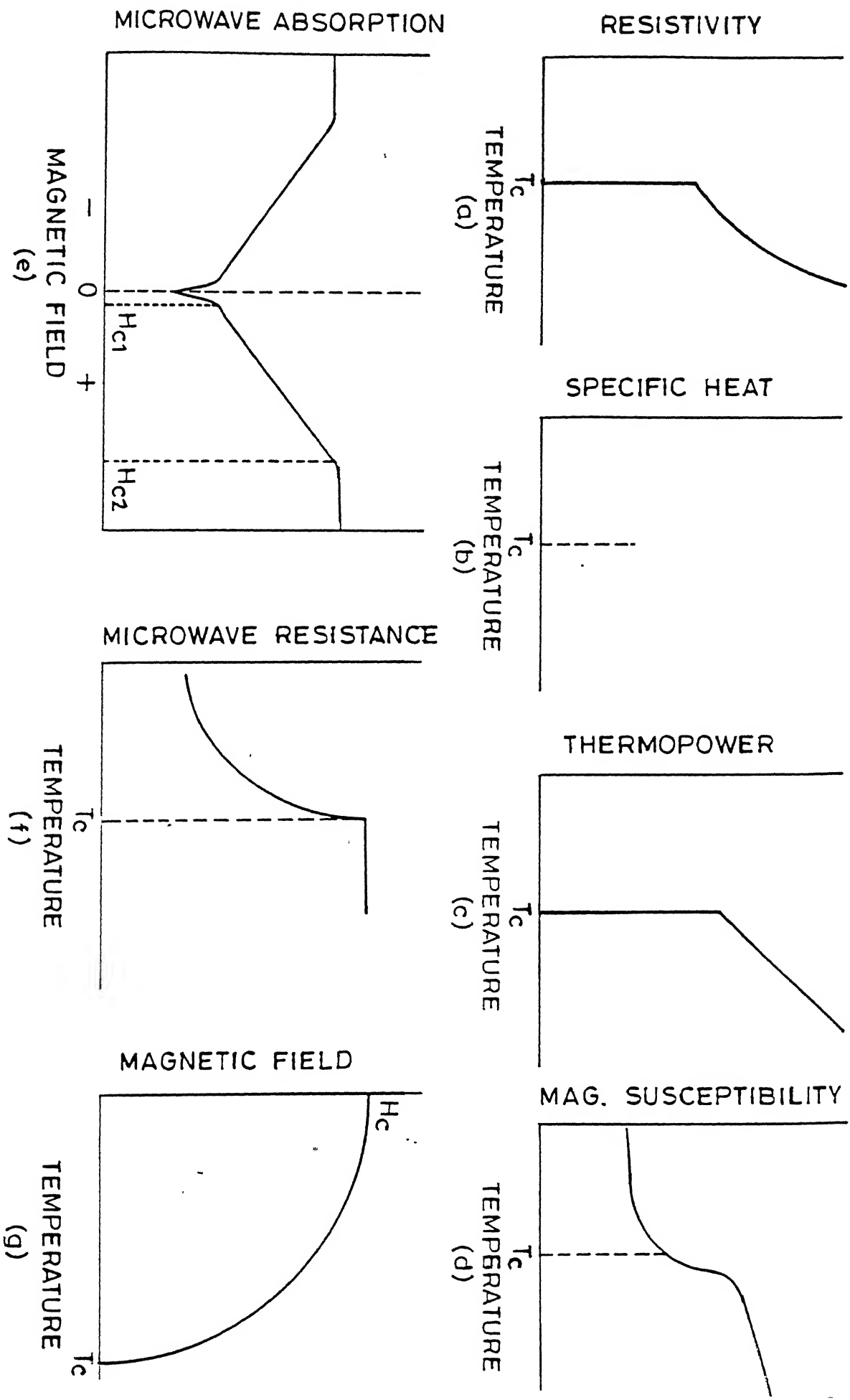


FIG. 1.2 SIGNATURES OF THE SUPERCONDUCTING STATE AND THEIR CONSEQUENCES.

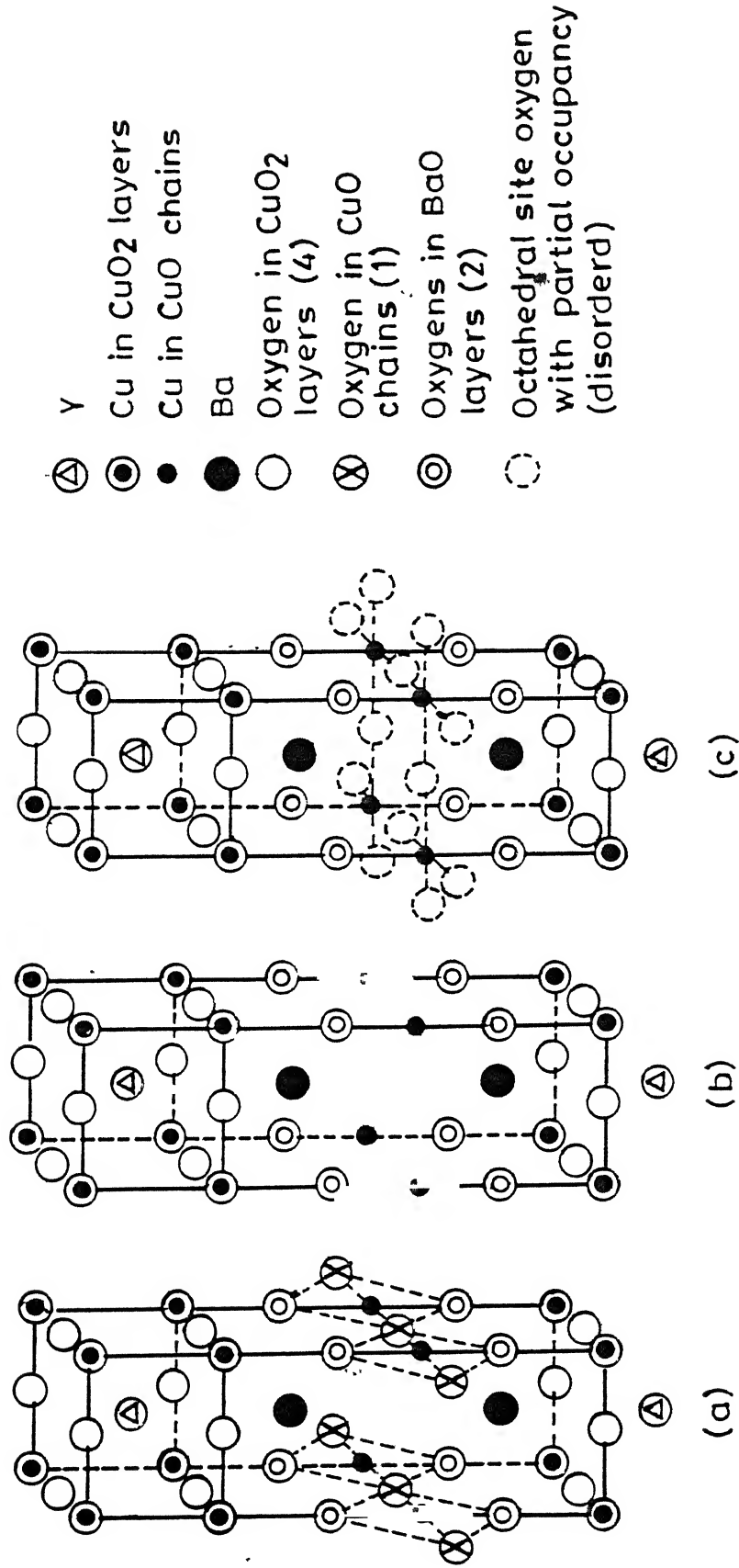


FIG. 1.3 STRUCTURES OF  $\text{YBa}_2\text{Cu}_3\text{O}_{7-\delta}$  (a) ORTHORHOMBIC STRUCTURE OF THE SUPERCONDUCTING PHASE WITH  $\delta \approx 0.0$ , (b) TETRAGONAL STRUCTURE OF THE NON SUPERCONDUCTING PHASE WITH  $\delta = 1.0$ , (c) DISTORTED STRUCTURE OF THE TETRAGONAL PHASE WITH  $\text{CuO}_6$  OCTAHEDRA WHERE SITE OCCUPANCY IS SMALL [AFTER CNR RAO]



## References

1. J.G. Bednorz, K.A. Muller, Z. Phys. B 64, 187, 1986.
2. M.K. Wu, J.R. Ashburn, C.J. Torng P.H. Hor, R.L. Meng, L. Gao, Z.H. Hung, Y.Q. Wang, C.W. Chu, Phys. Rev. Lett. 58, 908, 1987.
3. H. Maeda, M. Fukutomi, T. Asano, Jpn. J. App. Phys. Lett. 27, L209, 1988.
4. Z.Z. Sheng, A. M. Herman, Nature 332, 55, 1988 /332, 138, 1988.
5. W. Meissner, R. Ochsenfeld, Naturwissenschaften 21, 787, 1933.
6. F. London, H. London, Proc. Roy. Soc. Ser. A149, 72, 1935.
7. V.L. Ginsburg, L.D. Landau, JEPT 20, , 1064, 1950/A.A. Arbikosov, JEPT 32, 1442, 1957.
8. A.B. Pippard, Proc. Roy. Soc. Sr. A216, 547, 1956.
9. J. Bardeen, L.N. Copper, J.R. Schrieffer, Phys. Rev. 106, 162, 1987/ 108, 1175, 1957.
10. I. Giaever, Phys. Rev. Lett. 5, 147, 1960.
11. B.D. Josephson, Phys. Rev. Lett. 1, 251, 1962 /Adv. Phys. 14, 419, 1965.
12. D. Allender, J. Bray, J. Bardeen, Phys. Rev. B7, 1020, 1973.
13. C.M. Varma, S. Schmitt-Rink, E. Abrahams, Solid Stat. Comm. 62, 681, 1987.
14. T. Schneider, IBM J. Res. Dev. 33, 351, 1989.
15. C.M. Varma, IBM, J. Res. Dev. 33, 215, 1989.
16. Kamerlingh Onnes, Akad. van Wetenschappen ( Amsterdam), 14, 113, 818, 1911.

17. B.W. Roberts, Hand book of Chemistry and Physics, 61st Ed. E-87, 1980.
18. C.W. Chu, J. Bechtold, L. Gao, P.H. Hor, Z.J. Huang, R.L. Meng, Y.Y. Sun, YQ Wang Y.Y. Xue, Phys. Rev. Lett. 60, 941, 1988.
19. S.S.P. Parkin, Phys. Rev. B (Cond. matt.), 38(10), 6531, 1988.
20. T. Itoh, Jpn. J. App. Phys. Lett. 27(4), L559, 1988.
21. P.P. Freitas, C.C. Tsuei, T.S. Plaskett, Phy. Rev. B36, 833, 1987.
22. M. Hikita, M. Suzuki, Phy. Rev. B41, 834, 1990.
23. L.G. Aslamozov, A.I. Larkin, Fiz. Tverd. Tela 10, 1104, 1968. [Sov. Phy. Solid State 10, 875, 1968].
24. K. Maki, Prog. Theor. Phys. 39, 897, 1968 /40, 193, 1968., R.S. Thomson, Phys. Rev. B1, 327, 1970.
25. S.J. Hagen, Z.Z. Wang, N.P. Ong, Phy. Rev. B38, 7137, 1988.
26. T.C. Choy, M.P. Das, He Hong Xing, Physica C153-155, 671, 1988.
27. A.B. Kaiser, Phys. Rev. B37, 5924, 1988.
28. F.J. Blatt, P.A. Schroeder, C.L. Foiles, D. Greig, Thermoelectric Power of Metals (Plenum Press) New York, 1976.
29. M.A. Howson, M.B. Salamon, T.A. Friedmann, J.P. Rice, D.M. Ginsberg, Phys. Rev. B41, (1), 300, 1990.
30. K. Maki, J. Low Temp. Phys. 14, 419, 1974.
31. R.E. Prange, Phy. Rev. B1, 2349, 1970.
32. A. Schmid, Z. Phys. 215, 210, 1968/Phys. Rev. 180, 527, 1969/ Z. Phys. 229, 81, 1969.

33. S.D. Tyagi, Preprint: Invited talk at 1st Asia pacific Conf. on Cond. Matt. Physics, High Temp. Superconductivity and Related Topics - 27 june-3 july 1988, Singapore ( to be published by World Scientific).
34. S.D. Tyagi, M.Jeffery, C. Green, R. Gilmore , Phy. Rev. B39(13), 9054, 1989.
35. A Gould, Physica C 156, 555, 1988.
36. J.R. Schrieffer, "Theory of Superconductivity", Benjamin/Cummings Reading, Mass. 1964/1983.
37. V.L. Ginzburg, JEPT 20, 1549, 1965.
38. C.M. Varma, IBM, J. Res. Dev. 33(3), 215, 1989.
39. V.Z. Kresin, Phy. Rev. B35, 1987.
40. J.R. Schrieffer, X.G. Wen, S.C. Zhang, Phy. Rev. Lett. 60, 944, 1988 and references quoted therein.
41. P.W. Anderson, Science 235, 1196, 1987.
42. P.W. Anderson, G. Baskaran, Z. Zhou, T. Hsu, Phys. Rev. Lett. 58, 2790, 1987.
43. P. Prelovsek, T.M. Rice, F.C. Zhang, J. Phy. C20, L229, 1987.
44. L.J. De Jongh, Physica C 152, 171, 1988.
45. L. Liu, Solid Stat. Comm. 68(2), 269, 1988.
46. J. B. Goodenough and A. Manthiram in "Chemistry of Oxide Superconductors Ed. C.N.R. Rao, p-101, 1988.
47. A. Santoro, S. Miraglia, F. Beech, A. Sunshine, D.W. Murphy, L.F. Schneemeyer, J.V. Waszczak , Mat. Res. Bull. 22, 1009, 1987.
48. C.N.R. Rao, in "Chemistry of oxide superconductors" Ed. C.N.R. Rao, p-1, 1988.

49. P. Steiner, Z. Phys. B69, 449, 1988.
50. B. Douth, Z. Phys. B68, 407, 1987.
51. P. Sen, B. Dauth, T.Kachel, B. Rupp., W. Gudat, Physica C153-155, 153, 1988.
52. B.K. Chakravorty, D.D. Sarma, C.N.R. Rao, Physica C 156, 413, 1988.
53. Van der Laan, Phys. Rev. B23, 4369, 1981.
54. N.G. Stoffel, Phy. Rev. B36, 3986, 1987.
55. S. Sasaki, Z. Inove, N. Tyi, S. Takekawa, Jpn. J. App. Phy. 27(2), L206, 1988.
56. Z. Inove, S. Sasaki, N. Iyi, S. Takekawa, Jpn. J. App. Phy. 26, L1365, 1987.
57. S.X. Dou, H.K. Liu, A.J. Bourdillon, N. Sovvides, J.P. Zhov, C.C. Sorrel, Solid Stat. Comm. 68(2), 221, 1988.
58. D.D. Sarma, C.N.R. Rao, Solid Stat. Comm. 65, 47, 1988.
59. N. Murayama, E. Sudo, K. Kani, A.T. Suzuki, A. Kawakami, M. Awano, Y. Torii, Jpn. J. Appl. Phy. Lett. 27, L1623, 1988.
60. J. Kasperczyk, M. Piasecki, Z. Bak, Physica 153-155, 215, 1988.
61. M.W.C. Dharmawardana, Phys. lett. A. 126, 61, 1987 Phys. Rev. B36, 8873, 1987.
62. R.C. Budhani, S.M.H Tzeng, R.F. Bunshah, Phys. Rev. B36, 8873, 1987.
63. K.N.R. Taylor, D.N. Mathews, G.J. Russel, J. Crystaal Growth 85, 628, 1987.
64. S.R. Ovshinsky, R.T. Young, D.O. Alfred, G. de Maggio, G.A. von de. Luden, Phy. Rev. Lett. 58, 2579, 1987,
65. S.G. Eriksson, L.G. Johanson, C. Olsson, Physica C153-155, 902, 1988.

66. N.P. Bansal, D. Boyne, D.E. Farrell, J. Supercondu. 1(4), 417, 1988.
67. D.N. Matthews, A. Bailey, R.A. Vaile, G.J. Russell, K.N.R. Taylor, Nature, 786, 1987.
68. K.N.R. Taylor, A. Bailey, D.N. Matthews, G.J. Russell, Physica C153-155, 349, 1988.
69. D.N. Matthews, A. Bailey, G.J. Russell, J. Cochrane, R.A. Vaile, H.B. Sun, K.N.R. Taylor, Solid Stat. Comm. 65, 34, 1988.
70. T. Kato, Jpn. J. Appl. Phys. 27, L564, 1988.
71. P.H. Hor, R.L. Meng, Y.Q. Wang, L. Gao, Z.J. Huang, J. Bechtold, K. Forster, C.W. Chu, Phy. Rev. Lett. 58, 1891, 1987.
72. J.M. Tarascon, L.H. Greene, B.G. Bagley, W.R. McKinnon, P. Barboux, G.W. Hull in "Novel Superconductivity" eds. S.A. Wolf, V. Kreschnin, p-705 (Plenum Press) N.Y. 1987.
73. K.N. Yang, B.W. Lee, M.B. Maple, Appl. Phys. A46, 229, 1988.
74. K. Kinoshita, A. Matsuda, H. Shibata, T. Ishii, T. Watanabe, T. Yamada, Jpn. J. Appl. Phys. 27, L1642, 1988.
75. R.J. Cava, B. Batlogg, R.M. Fleming, S.A. Sunshine, Ramirez, E.A. Rietmann, S.M. Zahurak, R.B. Van Dover, Phy Rev. B37, 5912, 1988.
76. A. Tokiwa, Jpn. J. Appl. Phys. Lett. 27(6), L1009, 1988.
77. B. Okai, Jpn. J. App. Phys. Lett. 27(10), L1843, 1988.
78. S.K. Blower, Solid Stat. Comm. 68(8), 765, 1988.
79. I.S. Lyubultin, JEPT Lett. 47(4), 238, 1988.
80. A. Suzuki, Jpn. J. Appl. Phys. 27(5), L 792, 1988.
81. T. Komatsu, Jpn. J. Appl. Phys. Lett. 27(11), L2063, 1988.

82. M. Auslos, Solid Stat. Comm. 68(6), 539, 1988.
83. R. Liang, Physica C 157, 83, 1989.
84. S. Mazumdar, J. Phy. C 21(35), 5967, 1988.
85. B.W. Veal, W.K. Kwok, A. Umezawa, Appl. Phy. Lett. 51, 279, 1987.
86. J.M. Liang, J. Appl. Phy. 64(7), 3593, 1988.
87. Ki Hyun Yoon, Shung Sik Chang, J. Appl. Phys. 67(5), 2516, 1990.
88. A.S. Bhalla, R.Roy, L.E. Cross, "Chemistry of oxide superconductors, Ed. C.N.R. Rao, p-71, 1988.
89. B.A. Recherts, R.E. Allen, Phy. Rev. B37, 7496, 1987.
90. J.M. Tarascon, P.Barboux, P.F. Micelli, L.H. Greene, G.W. Hull, M. Eibschultz, S. A. Sunshine, Phys. Rev. B37, 7458, 1988.
91. P. Strobel, C. Paulsen, J.L. Tholence, Solid Stat. Comm. 65, 585, 1988.
92. G. Ferey, ALe Bail, Y. Laligand, M. Herriev, B. Reveau, A. Sulpice, R. Toumier, Solid Stat. Comm. 73, 610, 1988/ S.S. Michel, N.A. Mukhlif, Mat. Res. bull. 23, 1997, 1988.
93. A.F. Hepp, J.R. Gaier, P.D. Hambourger, J.J. Pouch in "Processing and applications of High Tc superconductors", Ed. M.E. Mayo, p-213, The Metallurgical Society, 1988.
94. M. Kuwabasa, N. kusaka, Jpn. J. Appl. Phys. 27(8), L1504, 1988.
95. X. Jian Sheng, C.Lie Zhao, F. Minghu, Z. Oirui, Z. Han, Q. Yitai, Solid Stat. Comm. 68(7), 643, 1988.
96. X. Jian Sheng, C. Lie Zhao, F. Minghu, Chin J. Low Temp. Phy. 11(5), 353, 1989.

- 97 S.P. Muntyan, G.A. Kioss, .... Physica Stat. Solidi, A114(1), K-63, 1989.
98. G. Xiao, Nature 332, 238, 1988/ Phys. Rev. Lett. 60, 1446, 1988.
99. Youwen Xu, Phy. Rev. B38(10), 7084, 1988.
100. T. Penney, Int. J. Mod. Phy. B2(5), 1235, 1988.
101. K.B. Lee, New Physics, (Korean Phy. Soc.), 28(5), 587, 1988.
102. R.F. Jordim, S. Gama, O.F. de Lima, S. Zacarelli, Solid Stat. Comm. 68(9), 835, 1988.
103. N. Ali, X. Zhang, P. Hill, S. Labroo, J. Less. Common Mat. 149, 435, 1989.
104. K. Okura, Jpn. J. Appl. Phy. Lett. 27(4), L655, 1988.
105. M. Itoh, Jpn. J. App. Phy. 27(9), L1634, 1988.
106. S. Kambe, M. Kawai, Jpn. J. Appl. Phy. 27(12), L2342, 1988.
107. Y. Hakwaku, F. Sunsiyashi, Phy. Rev. Lett. 58, 2579, 1987.
108. H. Fujii, H. Kowanaka, W. Ye, S. Orimo, H. Fukuba, Jpn. J. Appl. Phys. 27(4), 525, 1988.
109. I. Shih, C.X. Oiu, in "Processing and applications of High Tc superconductors". Ed. W.E. Mayo, p-223, The Metallurgical Society, 1988.
110. Y. Matsumoto, T. Abe, M. Tanaka, T. Tajawa, E. Sato, Mat. Res. Bull. 23, 1241, 1988.
111. G. Goldstone, M. A. Janson, J.R. Schieffer in "Superconductivity" Vol. 1, Ed. Parks, New York p-665, 1969.
112. C.U. Serge, Nature 329, 227, 1988.
113. R.J. Cava, B. Batlogg, C.H. Chen, E.A. Rictman, S.M. Zahurak, D. Werder, Phys. Rev. B36, 5719, 1987.
114. Z. Han, Chin, J. Low Temp. Phy. 11(5), 369, 1989.

115. T. Suzuki, J. Mat. Sci. Lett. 8, 11, 1271, 1989.
116. G. Baumgartel, K.H. Benneman, Phys. Rev. B40(10), 6711, 1989.



## CHAPTER - 2

## EXPERIMENTAL TECHNIQUES

## 2.1 Methodologies for Materials Preparation

For the preparation of the high  $T_c$  YBCO superconductor, three steps are essential :

- (i) a simultaneous or sequential but locally homogeneous reaction among the starting materials.
- (ii) the controlled nucleation of the desired crystallographic form, and
- (iii) the growth of these nuclei to the final microstructure.

These ingredients along with the experimental variables are best understood in terms of phase diagram of the system  $Y_2O_3$ -BaO-CuO.

2.11 Pseudoternary Phase Diagram of  $Y_2O_3$ -BaO-CuO System:

Fig. 2.1(a) shows the phase diagram for the system  $Y_2O_3$ -BaO-CuO at  $947^\circ C^{1, 2}$ , in which 123, 211 and 132 refer to  $YBa_2Cu_3O_{7-\delta}$ ,  $Y_2BaCuO_5$  and  $YBa_3Cu_2O_x$  respectively. The dashed line joining CuO to superconducting phase 123 is a joint at  $897^\circ C$  but is interrupted by melting at  $927^\circ C$ . The thick line shows a region of apparent solid solution and the dotted lines emanating from it reflect uncertainty in the end member composition. The 336 oxide  $Y_3Ba_3Cu_6O_{14}$  or the system  $Y(Ba_{2-x}Y_x)Cu_3O_7$  is also shown

in the diagram, although this is expected to be stable around  $847^{\circ}\text{C}$  or lower. Fig. 2.1(b) shows the phase diagram of the same system at  $967^{\circ}\text{C}$ <sup>3</sup>. This diagram is self explanatory.

Of the reported ternary phase diagrams, the area surrounded by  $\text{CuO-BaCuO}_2\text{-Y}_2\text{BaCuO}_5$  has been suggested to be important for the preparation of  $\text{YBCO}^{3-9}$ , as it contains the 123 phase. The  $\text{CuO-X}$  and  $\text{BaCuO}_2\text{-Y}$  vertical sections of the compatibility region are shown in Fig. 2.2(a) and (b), respectively. It can be seen that stoichiometric 123 phase will decompose incongruently into 211 and liquid phase. The melting process begins at about  $1010^{\circ}\text{C}$  and ends about  $1300^{\circ}\text{C}$  in air.

## 2.12 Sample Preparation

The three important techniques which have often been used to synthesize the high  $T_c$  superconductors are

- (i) Solid state reaction method
- (ii) Coprecipitation method, and
- (iii) Sol-gel technique

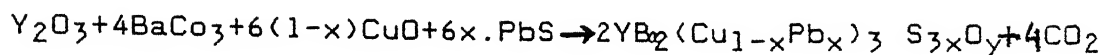
In the present work the samples have been prepared following the first method, viz. the solid state reaction technique, as described below.

The primary aim of the present work was to investigate the effects of partial substitution of PbS for CuO in YBCO superconductor. The starting materials used in this work are

- (i)  $\text{Y}_2\text{O}_3$  (IRE Ltd., India, 99.99%)
- (ii)  $\text{BaCO}_3$  (Qualigens Fine Chems, 99.99%)
- (iii) CuO (Alfa Products, USA, 99.99%) and

(iv) PbS (Alfa Products, USA, 99.99%)

The PbS doped YBCO samples were prepared in accordance with the following Solid state reaction.



Here x denotes the fractional partial substitution of CuO by PbS, and hence (100.x) directly gives the percentage substitution of PbS. In all, eight samples of compositions corresponding to x=0,0.005,0.01,0.02,0.05,0.08,0.1, and 0.2 were prepared in air. The appropriate amounts of starting materials were thoroughly mixed in a pestle and mortar and then pelletized at a pressure of  $\sim 6 \text{ ton/cm}^2$  into cylindrical pellets of diameter  $\sim 8 \text{ mm}$  and thickness around 4-5 mm. The pellets were heated at  $910-950^\circ\text{C}$  in a platinum boat for 15 hrs. and then cooled to room temperature. These pellets were reground into fine powder and pelletized at the same pressure as before and sintered once again at about the same temperature as earlier, but this time the retention time was kept around 18 hrs. The sintered pellets so obtained show a continuous colour change from black to greenish black as the doping concentration increases.

In addition, two more samples, corresponding to x=0.01 and 0.05 were also prepared by an alternative method; the pellets were sealed in evacuated quartz tubes. The heat treatment of both of these samples was done with the same ramps and retentions as for the first set of eight samples. The samples thus obtained had green colour.

CENTRAL LIBRARY

108883

The details of preparative parameters and codes of the samples with different compositions are listed in Table 2.1. One can readily see from this Table that as PbS concentration (x) increases the sintering temperature is decreased. This is so because the dopant PbS has a low melting point and hence its substitution in YBCO may lower the melting point of the resulting solid solution. The fact, that PbS doped YBCO samples fired at 950°C were found to be relatively hard burnt and non conducting, further substantiates the above argument.

## 2.2 Materials Characterization

The pure and PbS doped YBCO superconducting samples were characterized by XRD, SEM-EDX and resistivity measurements. The details of each of these is provided below.

### 2.21 X-Ray Diffraction (XRD)

The samples were examined by X-ray diffraction, using ISO Debye Flex Powder Diffractometer model 2002 from Rich and Seifert Co. FRG. The diffractometer uses  $\text{CuK}\alpha$  radiation ( $\lambda = 1.5418 \text{ \AA}$ ) obtained from a copper target using an inbuilt Ni-monochromating filter (density  $0.019 \text{ g/cm}^2$ , thickness  $0.021\text{mm}$ ). The diffractograms are taken in the range  $20^\circ \leq 2\theta \leq 70^\circ$  for all the samples, with the following recording conditions.

- (i) Sweep speed = 0.6 degree per min (in  $2\theta$ )
- (ii) Chart speed = 15 mm per min.
- (iii) Counts per min (CPM) = 10K
- (iv) Time constant. = 10 Sec.
- (v) Accelerating voltage = 80kV/20mA.

The existence of various peaks in the XRD pattern was used to identify the phases present in the sample. For pure YBCO sample, the diffractogram was indexed by using the method described by Warren<sup>12</sup>. The identification of extra phases in the doped samples was done by using the concept of Fink-indexing<sup>13</sup>.

To study the microscopic effect of doping in YBCO, it is often desirable to determine the effect of dopants on the lattice parameters. The lattice parameters may be determined by applying the d-spacing formula for orthorhombic structure (pure YBCO superconducting phase 123 has orthorhombic symmetry) to various reflections characterized by the (hkl) planes already indexed.

For orthorhombic symmetry the d-spacing formula is expressed as

$$1/d_{hkl}^2 = h^2/a^2 + k^2/b^2 + l^2/c^2 \quad \dots (1)$$

The effect of doping may also be realized in X-ray diffractograms in terms of the changes in relative intensities of some particular peaks. This type of analysis may also be applied to the evolution of extra phases as a function of doping.

## 2.22 Scanning Electron Microscopy - EDX Measurements

The scanning electron micrographs of the samples coated with gold were taken by the JEOL scanning electron microscope JSM-480A, equipped with a KEVEX ENERGY-DISPERSIVE X-RAY DETECTOR connected to a PC on which the KEVEX QUANTEX SOFTWARE is installed.

Operating the JEOL JSM-480A in ANALYTICAL mode and detecting the emitted X-ray by KEVEX detector, makes the quantitative elemental analysis of the sample possible. This type of analysis is generally referred to as energy dispersive X-ray microanalysis (EDX).

With the help of SEM micrograph of a sample displayed on video terminal, certain regions of interest are selected and the electron probe is allowed to fall on those regions one by one and corresponding EDX is acquired by QUANTEX facility available. In a typical EDX spectrum, to a first approximation, the height of a peak corresponding to an element is directly proportional to the amount of that element present in the sample. KEVEX software used in this study have special arrangements (commands) for the analysis of an EDX spectrum from a bulk material.

### 2.23 Resistivity Measurements

The standard Montgomery four-probe technique<sup>10,11</sup> with equi-probe distance configuration is used to determine the resistivity of the samples as a function of temperature. This method permits the measurement of resistivity of a sample in the shape of a rectangular bar with the dimensions, say,  $a \times b \times c$ ,  $a$  and  $b$  being the two larger dimensions and  $d$  the thickness of the bar. If the four-probes, having very small contact areas with the surface, rest on the  $a$ - $b$  plane of the sample as shown in Fig. 2.3,  $l_1$  and  $l_2$  being the probe distances, the resistivity may be expressed as

$$\rho = K d_{\text{eff}} \cdot R \quad \dots (1)$$

where  $K$  is a function of  $l_2/l_1$  as given in following table,  $d_{eff}$ , the effective thickness of the sample which may be determined using Fig. 2.3, and  $R$  is the ratio of the floating voltage  $V$  to the probe current  $I$ .

Selected Values of Function  $K$

$l_2/l_1$	0.25	0.5	0.6667	1.0	1.5	2.0	4.0
$K$	0.3207	0.8911	1.562	4.531	21.86	105.1	56300.0

This method is especially useful in measuring resistivity as a rapidly varying function of temperature as is the case in the present studies.

The basic cryogenic system APD superconductor characterization cryostat from APD Cryogenics, Inc., is used in these measurements. This system is based on the principle of closed cycle refrigeration. Helium is used as the refrigerant charge. The unit consists of a compressor module (APD-HC-2), an expander module and the interconnecting hoses to carry refrigerant between the two modules. In addition to compressing and recycling the refrigerant charge, the compressor module cools

and cleans the refrigerant to remove any oil and residual water vapour. The system uses two hoses; one to carry high pressure helium to the expander and the other for returning the low pressure gas to the compressor.

The expander module APD, DE 202 is the heart of the system, it is a two stage cryogenic refrigerator, using gaseous Helium as the refrigerant, powered and controlled by a compressor module. The compressor module also supplies the required gaseous Helium. The schematic diagram of expander module is shown in Fig. 2.4. The sample under investigation is placed in the second regenerator stage. Two temperature sensors (silicon diodes) are used. One is placed in the first stage while the other in the second; very close to the sample. For precise temperature indication and control the system is equipped with a microprocessor-based temperature indicator-cum-controller model 5500-1-25 from Scientific Instruments Inc. USA.

Four point contacts on well polished and cleaned surface of the samples are made by placing four very small dots of silver paint (composition 1220-C Elteks Bangalore) as shown in Fig. 2.3. The point contacts are made conducting and mechanically enduring by curing at  $\sim 100^{\circ}\text{C}$  in air for  $\sim 2$  hrs, followed by cooling to room temperature inside the oven. Now four thin copper wires are stuck to the four points using again the same silver paint. The sample is subjected to the same curing as earlier. The contacts were checked at room temperatures before loading the sample in the sample-holder for resistivity measurement. The contact resistance at room temperature was usually found to be less than 1 ohm.



For four-probe resistivity measurements, a precision constant current source (Knick, FRG, model JS-300) was used to supply the probe current  $I$ . The value of  $I$  was usually 10 mA. The floating voltage  $V$  was measured by digital nanovoltmeter (Keithley model 181). The floating voltages were also read by changing the direction of current, in order to avoid possible geometrical and thermoelectric errors. The average of the two readings was taken as the value of floating voltage, and then resistivities at various temperatures were calculated as described earlier.

The modern trend is to analyse the resistivity data in terms of normalized resistivity, as it represents the inherent property of the sample material and excludes all the experimental errors. The normalized resistivity is found by taking the ratio of resistivity at temperature  $T$  to that at room temperature ( $\rho(T)/\rho(300)$ ). Thus if  $V_T$  is the floating voltage at any temperature ( $T$ ) corresponding to a constant current  $I$ , the resistivity  $\rho(T)$  may be written as :

$$\rho(T) = K_{\text{eff}} \cdot (V_T/I) \quad \dots (2)$$

and at room temperature (300K) the resistivity is given by

$$\rho(300) = K_{\text{eff}} \cdot (V_{300}/I) \quad \dots (3)$$

And hence the normalized resistivity at temperature  $T$  may be written as

$$N\rho = \rho(T) / \rho(300) = V_T / V_{300} \quad \dots (4)$$

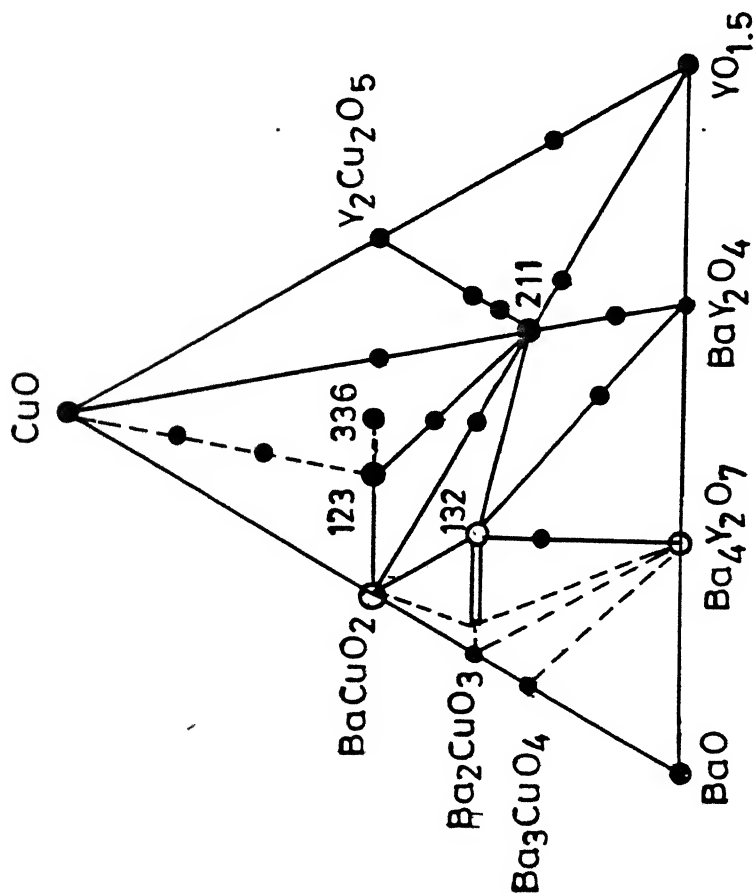
Which is clearly free from geometrical factors  $K$  and  $d_{eff}$  and the current  $I$ . The normalized resistivities for all samples were directly calculated by dividing the floating voltages at different temperatures by the floating voltage at 300K. However, the room temperature resistivities  $\rho(300)$  of the samples were determined using equation (1).

Table 2.1

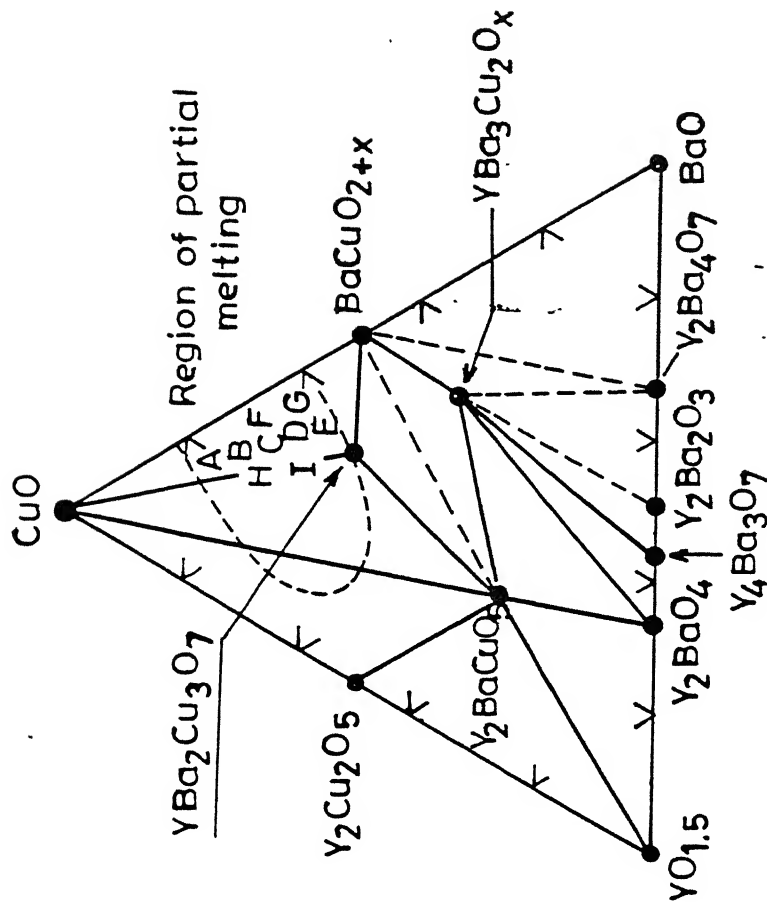
The preparational details of PbS doped YBCO samples

Fractional substi- tution* (x)	Preparative Conditions			Sample code
	Ramp.(Sintering temperature( $^{\circ}$ C)	Retention times(hrs.) 1st firing/ 1Ind firing	Atmosphere air/vacuum	
0.00	950	15/18	air	AK02T
0.005	945	15/18	air	AK04T
0.01	935	15/18	Vacuum (eva- cuated sealed Quartz tube)	AK10T
			air	AK11T
0.02	935	15/18	air	AK12T
0.05	920	15/18	Vacuum (eva- cuated sealed Quartz tube)	AK09T
			air	AK03T
0.08	920	15/18	air	AK15T
0.1	910	15/18	air	AK16T
0.2	910	15/18	air	AK17T

\* x in  $\text{YBa}_2(\text{Cu}_{1-x}\text{Pb}_x)_3\text{S}_{3-x}\text{O}_y$

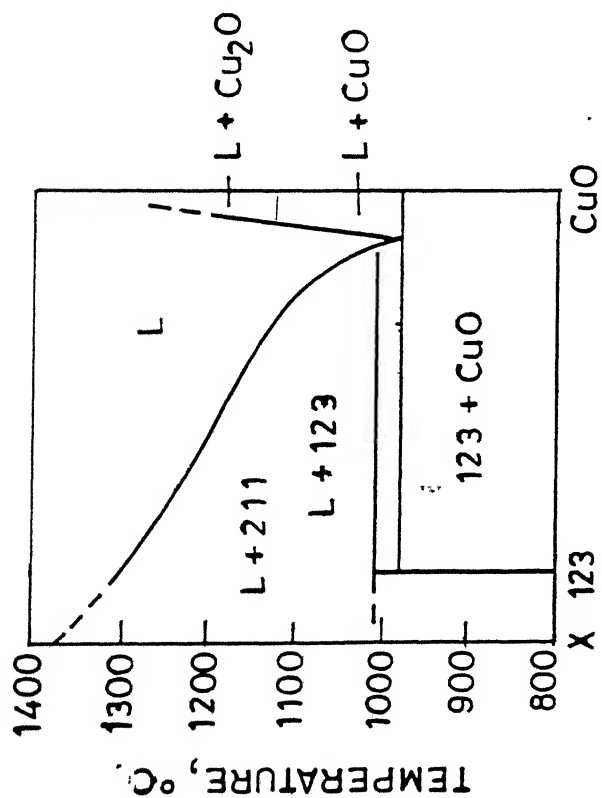


(a) 947°C

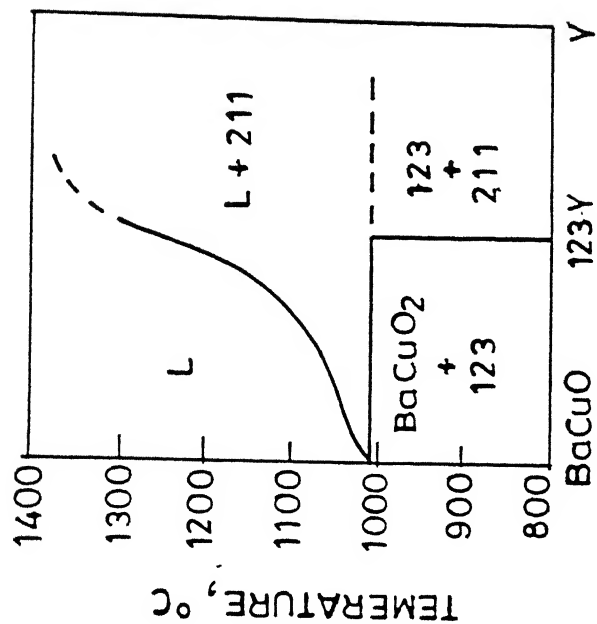


(b) 967°C

FIG. 2.1 PSEUDO-TERNARY PHASE DIAGRAM OF THE  $Y_2O_3$  -  $BaO$  -  $CuO$  SYSTEM.



(a)



(b)

FIG. 2.2 CuO-X (a) AND BaCuO<sub>2</sub>-Y (b) VERTICAL SECTIONS OF BaCuO<sub>2</sub>-211-CuO TRIANGLE IN YBCO PSEUDO-TERNARY PHASE-DIAGRAM.

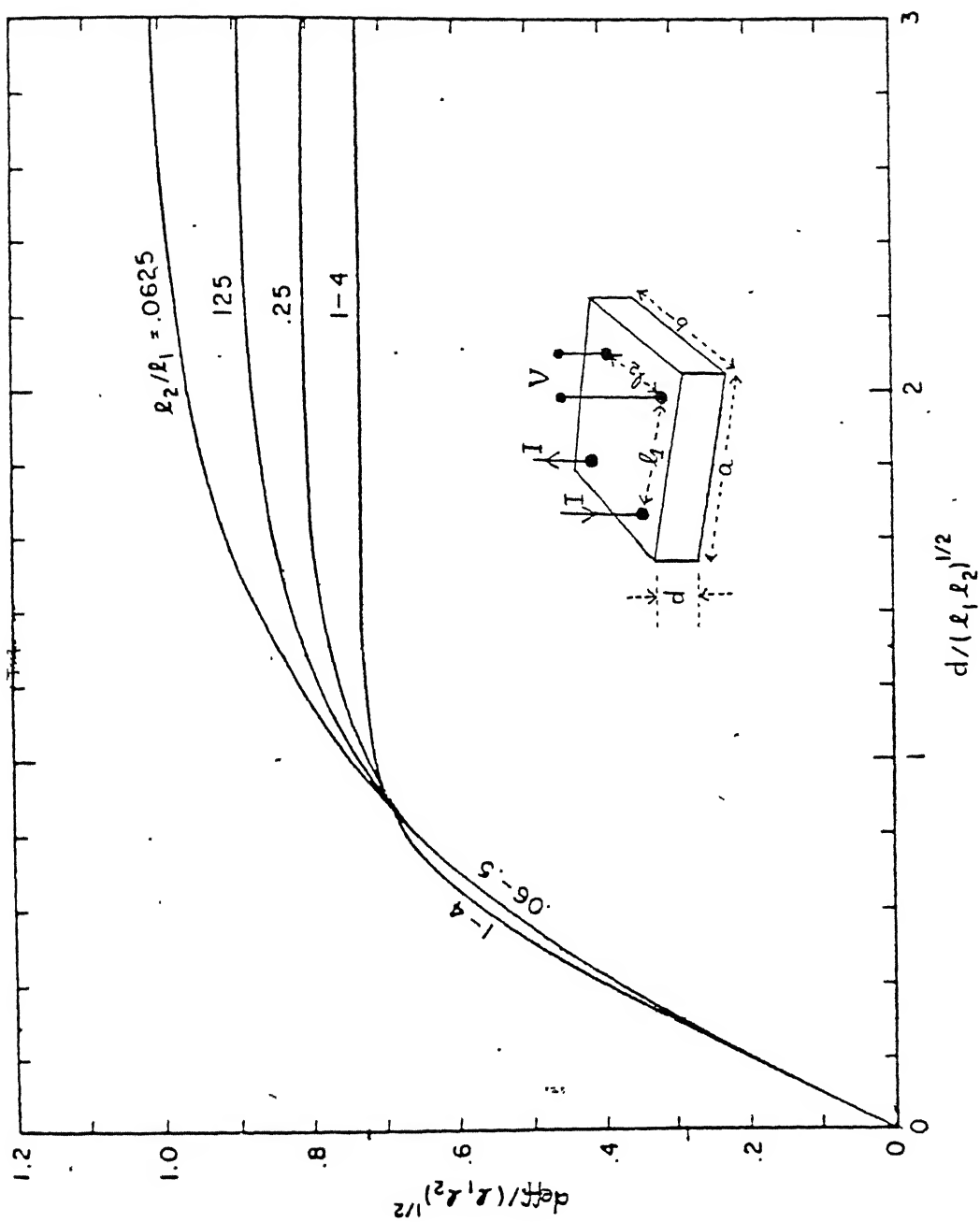
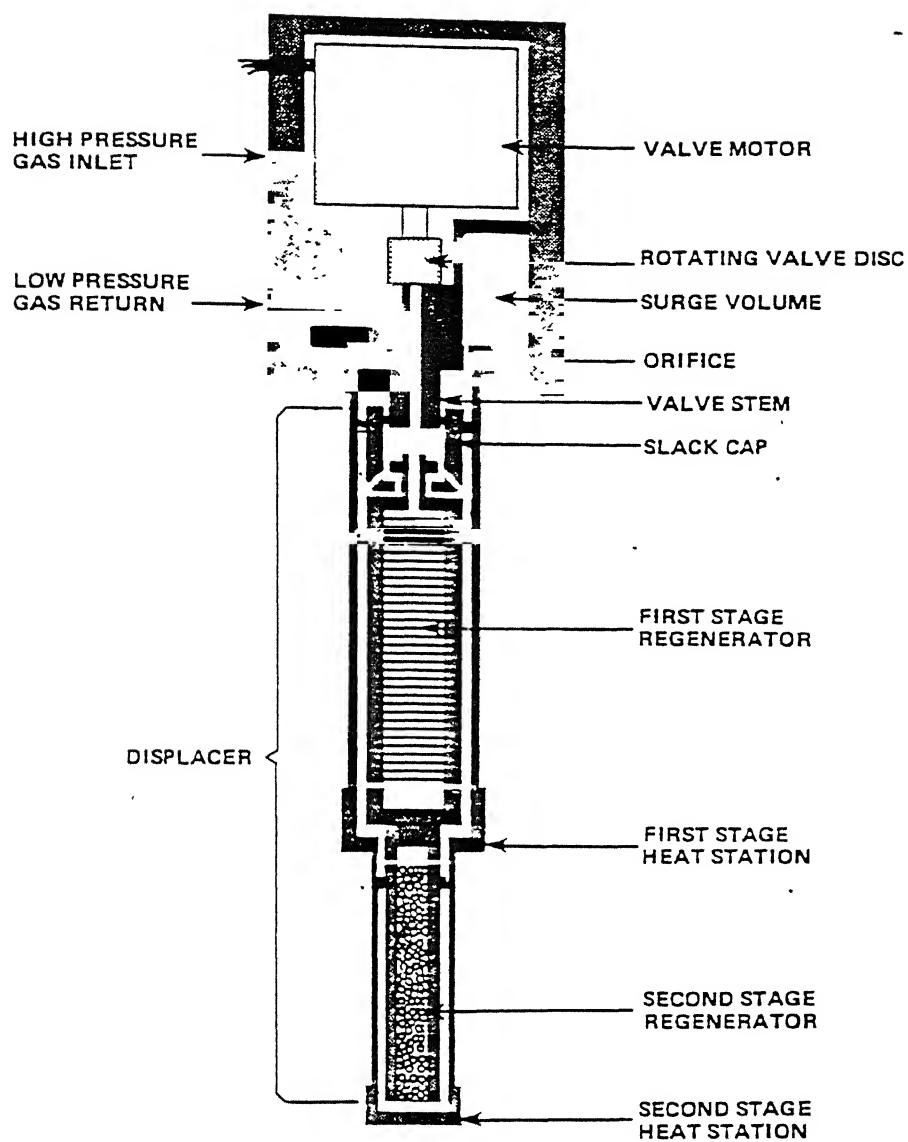


FIG.2.3: DEPENDENCE OF EFFECTIVE THICKNESS  $d_{eff}$  ON PROBE-DISTANCE



**FIG.2.4: SIMPLIFIED EXPANDER MODULE DIAGRAM.**

## References

- (1) C.N.R. Rao, J. Solid Stat. Chem., 74, 147, 1988.
- (2) D.R. Clark, Int. J. Mod. Phys. B1, 170, 1987.
- (3) R.S. Roth, Adv. Ceram Mater. 2, 303, 1987.
- (4) S. Takekawa, N. Iyi, Jpn. J. Appl. Phys. 26, L851, 1982.
- (5) L.F. Schneemeyer, J.V. Waszczak, T. Siegrist, R.B. Van-Dover, L.W. Rupp., B. Batlogy, R.J. Cova, D.W. Murphy, Nature, 328, 601, 1987.
- (6) D.L. Kaiser, F. Holtzberg, B.A. Scott, T.R. Mc. Guire, Appl. Phys. Lett. 51, 1040, 1987.
- (7) D.L. Kaiser, F. Holtzberg, M.F. Chisholm, T.K. Worthington, J. Cryst. Growth, 85, 593, 1987.
- (8) R.A. Laudise, L.F. Scheemeyer, R.L. Barns, J. Cryst. Grow. 85, 569, 1987.
- (9) K. Oka, K. Nakane, M. Ito, M. Saito, H. Unoki, Jpn. J. Appl. Phys. 27(6), L1065, 1988.
- (10) H.C. Montgomery, J. Appl. Phys. 42(7), 2971, 1971.
- (11) B.F. Logan, S.O. Rice, R.F. Wick, J. Appl. Phys. 42(7), 2975, 1971.
- (12) L.V. Azaroff, "Elements of X-Ray Crystallography", Mc Grow Hill Book Company 1968.
- (13) B.E. Warren, "X-Ray Diffraction", Addison Wesley Publishing Company 1969.



## RESULTS AND DISCUSSION

High  $T_c$  oxide superconductors with nominal composition  $YBa_2(Cu_{1-x}Pb_x)_3S_{3x}O_y$  were synthesized from stoichiometric amounts of  $Y_2O_3$ ,  $BaCO_3$ ,  $CuO$  and  $PbS$ , as described in Section 2.1. Eight samples corresponding to  $x=0, .005, .01, .02, .05, .08, .01$  and  $0.2$  were prepared in air. The details of preparative aspects and labeling of samples are described in Table 2.1. It was observed that the samples with higher dopant concentration ( $x$ ) of  $PbS$  got better sintered leading to larger reduction in the size. The basic features developed as a result of this improved sinterability are similar to those observed in  $KCl$  doped<sup>1</sup>  $YBCO$ . A maximum shrinkage of about 12.5% was observed for the sample with  $x=0.2$ . Extended exposure of the sample to the atmosphere appeared to degrade the surfaces of the sample as evidenced by a change of colour ;probably due to formation<sup>2</sup> of barium carbonate and/or hydroxides. The samples prepared in the evacuated sealed quartz tube however, do not show this effect. The structural characterization of these samples was done using XRD and SEM-(EDX), while the superconducting properties were investigated by resistivity measurements.

## 3.1 X-Ray Diffraction (XRD)

The XRD patterns for all the ten samples (eight samples with  $x=0, .005, .01, .02, .05, .08, 0.1$  and  $0.2$  prepared in air and two samples with  $x=.02$  and  $.05$  prepared in evacuated sealed

quartz tube) were recorded at room temperature. The details of the recording conditions such as chart speed, wavelength of the radiation used, etc. are given in Section 2.21 (Chap. 2). Both the samples prepared in evacuated sealed quartz tube were found to be insulators. The XRD patterns for these samples also did not show peaks either corresponding to orthorhombic or tetragonal phase of YBCO.

Fig. 3.1 shows the XRD patterns of some selected samples prepared in air. The XRD results for  $x=0$  sample show peaks that can be attributed to superconducting orthorhombic phase, and there are no peaks to suggest the presence of any impurity (second) phase in appreciable quantity. Table 3.1 summarizes the  $2\theta$  values of various peaks and the corresponding  $(hkl)$  and their interplanar spacing,  $d_{hkl}$ , alongwith the relative intensities of the peaks.

The XRD patterns for the sample with  $x=.005$  (not shown in Fig. 3.1) were found identical to that of  $x=0$  (pure samples). However, as the concentration ( $x$ ) of the dopant (PbS) increases, extra lines in the XRD patterns appear suggesting the presence of impurity phase(s). For example, the XRD patterns corresponding to  $x=0.01$  and  $.02$  show an extra peak, in addition to those attributable to orthorhombic YBCO phase, at  $2\theta = 29.6^\circ$  that may be attributed to  $Ba_3Y_4O_9$  or  $Y_2BaCuO_5$ . However, the EDX analysis of these samples to be discussed later point out that the impurity phase present is probably  $Y_2BaCuO_5$  rather than  $Ba_3Y_4O_9$ . The evolution of this impurity phase has also been reported in various doped YBCO<sup>3,4</sup> superconductors also. The intensity data given in Table 3.2 would clearly indicate that as the dopant

concentration increases, the amount of the impurity phase also increases. The results for  $x=.02$  sample show one more extra peak at  $2\theta = 52.2^\circ$  which has been attributed to the presence of  $\text{BaPbO}_3$ . The same impurity has also been found in Pb doped 5.6 YBCO samples. Apart from this, the XRD patterns for  $x=.01$  and corresponding to the primary orthorhombic phase has decreased for  $x=.02$  sample.

The XRD pattern for  $x=0.05$  sample is somewhat anomalous in two respects : First, the heights of various peaks corresponding to the main (orthorhombic YBCO) phase have increased in comparison to those of  $x=.01$  and  $.02$  samples. Second, the height of the peak at  $2\theta = 29.6^\circ$  corresponding to the impurity (second) phase,  $\text{Ba}_3\text{Y}_4\text{O}_9$  or  $\text{Y}_2\text{BaCuO}_5$ , has decreased in comparison to those of  $x=0.01$  and  $0.02$  samples. This would immediately suggest that the sample with  $x=.05$  has larger fraction of orthorhombic YBCO phase than those with  $x=.01$  and  $.02$  samples. This is a somewhat surprising result particularly because the samples with  $x=.01$  and  $.05$  were prepared simultaneously under the same conditions, and hence the observed anomaly can not be explained in terms of differing preparational conditions.

The XRD patterns for sample with  $x=.08$  shown in Fig. 3.1 are essentially similar to those of  $x=.01$  and  $.02$  samples except that the peaks corresponding to the second phase are more pronounced in the former. The XRD results for  $x=0.1$  sample show several extra peaks (see Table 3.1) suggesting that the volume fraction of the main orthorhombic superconducting phase has decreased considerably. The resistivity results which will be

discussed later are consistent with the XRD data in the sense that the samples with  $x=.08$  and  $0.1$  are no longer metal-like but have become semiconductor-like. The same type of results have been reported<sup>7-9</sup> in YBCO samples doped with isovalent transitional elements in place of copper.

The XRD results for  $x=0.2$  sample show prominent peaks corresponding to the impurity phase(s) indicating that the concentration of the orthorhombic phase has decreased significantly. The resistivity data showed that this composition was more like an insulator.

To summarize the XRD results, the composition with  $x=0$  and  $0.005$  are single phase (orthorhombic YBCO). As  $x$  increases further, the material becomes multiphasic and the volume fraction of the superconducting ortho-phase decreases continuously as revealed by the decreased intensity of the peaks corresponding to ortho-phase. The only exception to this is the sample with  $x=.05$ . The sample with highest dopant ( $x=0.2$ ) probably contains so little of ortho-phase that it is like an insulator.

An interesting fact revealed by the XRD results is that none of the possible impurity phases identified by us contains sulphur. This implies that all the sulphur of doped PbS has gone into the lattice of YBCO phase. Another evidence for this is the increase in the intensity of reflection<sup>10</sup> corresponding to the plane (005) of the superconducting phase as the dopant concentration increases from  $x=0$  to  $x=.05$  (Fig. 3.1 and Table 3.1). However, the composition dependence of the intensity of the impurity phase  $\text{BaPbO}_3$  (Table 3.2) predicts that Pb forms the  $\text{BaPbO}_3$ , rather than substituting Cu completely. This would

suggest that only a part of Pb (out of doped PbS) substitutes for Cu, while all the sulphur gets into the lattice. This latter is further supported by the evidence that there was slight expansion of c-axis, probably due to incoming large S ions. These observations about the selective intake of sulphur from PbS into YBCO matrix are consistent with the reports<sup>11,12</sup> dealing with direct sulphur substitution in YBCO.

### 3.2 Scanning Electron Microscopy (SEM)-EDX Analysis

All the samples were examined by SEM and also selected portions of the samples analysed by energy dispersive X-ray micro-analysis (EDX). Plates 3.1 to 3.4 show the microstructure of some selected samples. It is evident that the grain size increases (plates 3.1 to 3.3) as the concentration (x) of PbS increases in the matrix, suggesting that the PbS also acts as a sintering agent, such as a liquid medium. However, as x exceeds 0.05 the grain size starts decreasing (Plate 3.4) perhaps owing to the formation of the second (impurity) phase excessively. The effect is similar to that observed<sup>13</sup> in the Au substituted YBCO. The microstructural observations show that the addition of PbS eliminates or minimizes the cracks and promotes the grain growth due to liquid phase sintering.

The SEM micrographs shown in Plates 3.2-3.4 reveal the presence of :

- (i) a dark phase (labeled C in Plate 3.2 or labeled A in Plate 3.3) is the matrix (superconducting ortho-phase).
- (ii) a bright phase (labeled A in Plate 3.2 or C in Plate 3.3) is the impurity phase distributed randomly, and

(iii) a gray phase (labeled B in Plate 3.2) is a second impurity phase.

It is concluded from these studies that the lightly doped samples are largely single ortho-phasic, while the samples with larger dopant concentration are mixtures of two or even three phases as mentioned above. The studies<sup>4,14</sup> dealing with the mixed phase YBCO oxide superconductors strengthen the above description of phases.

The EDX analysis ( Figs. 3.2-3.5) of the aforesaid phases, viz. the matrix or the ortho-phase, the first (bright colour) impurity phase and the second (gray) phase, revealed the following chemical constitution.

---

Phase	Constitution (EDX Analysis)	Expected Constitution
Matrix (Ortho-Phase)	$Y_{16.5}Ba_{36.9}Cu_{46.5}O_Y$	$YBa_2Cu_3O_7$
Bright impurity phase	$Y_{56}Ba_{26}Cu_{22}O_Y$	$Y_2BaCuO_5$
Gray impurity phase	$Y_{5.7}Ba_{49.7}Cu_{44.5}O_Y$	?

---

The samples with larger dopant concentration ( $x \geq .01$ ) showed the presence of S in the main (matrix) phase indicating that S probably has substituted for O in the ortho-phase. Further the EDX analysis (Fig. 3.3) shows that the main impurity phase is probably  $Y_2BaCuO_5$ . It should, however, be pointed out that the chemical composition of the second gray-impurity phase varied considerably from one sample to the other. The lightly doped samples did not show the presence of any Pb in this impurity phase (Fig. 3.4). On the other hand samples with  $x \geq 0.02$  showed almost negligible concentration of Cu (Fig. 3.5).

Thus the XRD and the SEM-EDX studies lead to the following conclusions:

- (1) The samples with  $x=0$  and  $0.005$  showed the existence of one phase only, viz. the superconducting ortho-phase.
- (11) The samples with higher dopant concentration ( $x \geq .01$ ) showed the presence of impurity phases varying in number, chemical composition and volume fractions. For example, the sample with  $x=.2$  showed at least 3/4 impurity phases in such large quantities that the superconducting ortho-phase became the minor constituent.
- (111) Most of the sulphur out of the dopant  $PbS$  has substituted for oxygen in the ortho-phase, but only a small fraction of Pb probably substitutes for Cu and a larger fraction is found segregated near grain boundaries<sup>15</sup> as a part of the impurity phase.

### 3.3 Resistivity Measurements

Electrical resistivity was measured by four probe technique as described in Chapter 2. The two samples of nominal compositions  $\text{YBa}_2(\text{Cu}_{1-x}\text{Pb}_x)_3\text{S}_x\text{O}_y$  ( $x=.01$  and  $0.05$ ) prepared in evacuated sealed quartz tubes were found insulators contrary to that reported by Harrison et al<sup>16</sup>, and hence this method was discarded for any further preparation of high  $T_c$  superconductors. The samples were subsequently prepared and sintered in air.

Fig. 3.6 shows the normalized resistivity ( $N \rho_{90}$ ) as a function of temperature (K) for all the seven superconducting samples of compositions corresponding to  $x=0, .005, 0.01, 0.02, .05, .08$  and  $0.1$ . The anomalous temperature dependence<sup>17</sup> of resistivity in various samples show a relation with composition ( $x$ ). It is observed that the samples containing a dopant concentration of upto  $0.05$  show a metallic behaviour above  $T_c$ . However, as  $x$  increases, the room temperature resistivity,  $\rho(300)$ , first decreases upto  $x=.01$  and then starts increasing rapidly. It has already been pointed out that the sample containing highest dopant concentration ( $x=0.2$ ) eventually becomes insulator. The samples with  $x=0.08$  and  $0.1$  are, however, semiconductor-like, i.e. the  $\rho$  increases as temperature decreases ( $d\rho/dT = -ve$ ). The room temperature resistivities alongwith  $(d\rho/dT)N$ ,  $T_c$  and  $\Delta T_c$  are listed in Table 3.3. One can easily see that this trend of variation in properties is almost similar to the variation caused by the transition metal substituents at Cu sites<sup>5,18-20</sup>. However, a sudden dip in  $\rho(300)$  is analogous to the one reported by Bansal et al<sup>21</sup> and Rao et al<sup>22</sup> in a sulphur substituted YBCO compound.



Thus the PbS doped YBCO showed the properties, that are the mixture of the properties of both transitional metal substituted and sulphur substituted products.

Fig. 3.7 shows the normalized resistivity vs. temperature around the critical region (80-95K) for the first five samples which were found to exhibit normal metallic character at  $T > T_c$ . In general, the  $T_c$  decreases as the dopant concentration ( $x$ ) increases except a minor anomaly associated with  $x=0.02$  sample which shows a slightly higher  $T_c$  than that for  $x=0.01$  sample. A similar increase in  $T_c$  has also been reported in Co and Ni substituted YBCO<sup>23,24</sup> samples almost at the same composition ( $x$ ). As far as the transition width ( $\Delta T_c$ ) is concerned, it initially decreases (upto  $x=0.01$ ) and then starts increasing beyond  $x=0.02$ .

For a more precise determination of  $T_c$  and  $\Delta T_c$  a computer program was developed which permits the determination of  $d\rho/dT$ ,  $d^2\rho/dT^2$ , excess conductivity or paraconductivity ( $P$ ,  $\Sigma$ ), at a desired temperature interval and over a selected temperature range from the raw data of  $\rho$  vs.  $T$ . The  $d\rho/dT$  data so obtained at a temperature interval of 0.5K is plotted as a function of temperature in the critical region, and the results are shown in Fig. 3.8. It is evident that  $d\rho/dT$  vs.  $T$  curve exhibits a sharp maximum. The location of the maximum was taken as  $T_c$ <sup>25,26</sup> and the width at half maximum is taken as the transition width ( $\Delta T_c$ )<sup>25</sup>. The  $T_c$ 's and  $\Delta T_c$ 's obtained in this manner are listed in Table 3.3. As has already been pointed out, the  $T_c$  generally decreases as the dopant concentration( $x$ ) increases with the exception of one sample with  $x=0.02$ . However, there is no discernible effect of doping on the transition width which for

most samples was found to lie in the range 1.5-2.2K except for one sample with  $x=0.01$ , which showed  $\Delta T_c$  as low as 0.8K. This result is consistent with those quoted by Kambe and Kawai<sup>11</sup> for chalcogen doped YBCO-ortho phase.

The excess or para-conductivity ( $P\sigma$ ) and the reduced temperature,  $\epsilon = (T-T_c)/T_c$ , are related through the following equation

$$P\sigma = K \epsilon^n \quad \dots\dots (1)$$

where,  $K = (e^2 / 32\hbar) \xi(0)^{-1}$ ,  $n = -1/2$  .....for 3D

$K = (e^2 / 16\hbar) \cdot (1/d)$ ,  $n = -1$  .....for 2D

and  $K = (\pi/16) \cdot [e^2 \xi(0)/\hbar S]$ ,  $n = -3/2$  .....for 1D

where  $\xi(0)$  is coherence length<sup>28</sup>,  $d$  the characteristic length in 2-D system<sup>29</sup>,  $S$  the cross sectional area and the other symbols have their usual meaning.

Thus both  $K$  and  $n$  are the parameters which depend upon the dimensionality of the superconductor and its nature<sup>30</sup>.  $K$  is related to characteristic lengths  $\xi(0)$  or  $d$  depending on the dimensionality<sup>29</sup> of the superconductor and hence it is often called characteristic length parameter. The exponent  $n$  of Equation (1) is related to the fluctuation effects<sup>31</sup> above  $T_c$  and hence to the fluctuation conductivity, and is generally called the paraconductivity exponent or the superconducting order parameter.

The normalized paraconductivity ( $NP\sigma$ ) at any temperature defined as the ratio of paraconductivity to the room temperature conductivity ( $\sigma_{300}$ )<sup>31</sup> may be expressed as:

$$NP\sigma = P\sigma / \sigma_{300} = (K / \sigma_{300}) \cdot e^n \quad \dots (2)$$

$$\text{or,} \quad \ln (NP\sigma) = \ln (K / \sigma_{300}) + n \ln e \quad \dots (3)$$

Thus a plot between  $\ln (NP\sigma)$  and  $\ln e$  should be a straight line<sup>27</sup> whose slope should yield the paraconductivity exponent ( $n$ ), and the intercept yields the parameter  $K$ .

Fig. 3.9 shows the plots of  $\ln (NP\sigma)$  vs.  $\ln e$  for all the five samples which showed metallic behavior at  $T > T_c$ , viz.,  $x=0$ , 0.005, .01, .02 and .05. The order parameter ( $n$ ) and the characteristic length parameter ( $K$ ), as determined from the Fig. 3.9, are plotted as a function of composition ( $x$ ) in Fig. 3.10. It is observed from Fig. 3.10 that both  $K$  and  $n$  decrease initially, going through a minimum at  $x = 0.005$  and then start increasing rather rapidly in the range  $x > 0.01$ . The specific values of  $K$  and  $n$  are listed in Table 3.4. The pure sample shows a 3-D behavior ( $n = -1/2$ ). However, as the dopant concentration increases, the dimensionality changes from 3 to 2. To the best of our knowledge there are no reports of crossover of the dimensionality from 3 to 2 as a result of doping effects. However, the result that pure YBCO shows 3D - superconductivity near  $T_c$  is consistent with the results of previous studies<sup>25,27,32</sup>. The 3D to 2D cross over observed in the present study as a result of doping may not be attributed to the

processing parameters, as the effects on exponent  $n$  caused by these are very small<sup>25,27</sup>. However this result may appear to bear an indirect correlation with the results observed in resistivity measurements in presence of magnetic field.<sup>5,30,33</sup>. The cross over observed due to magnetic field quenching<sup>34</sup> is treated theoretically by Maki and Thomson<sup>35</sup> and Arnov et al<sup>36</sup>. One can easily realize the equivalence of the two phenomenon, viz. the cross-over due to magnetic field and that due to doping, just by comparing the results. So it is reasonable to say that effect of PbS doping is similar, in some ways, to the application of a magnetic field. This suggests an explanation of the effects observed in terms of the presence of a field inside the doped compound probably due to the specific sites taken by the dopant atoms.

The other important feature observed in PbS doped YBCO system is the unique trend of variation of  $T_c$ . The lowering of  $T_c$  may be attributed to the presence of the impurity phases<sup>6,37</sup> due to doping. The slight increase in  $T_c$  at  $x=.02$  is probably the effect of sulphur addition<sup>10,38,39</sup>. Thus this unique trend in variation of  $T_c$  may be considered as an interplay between the two opposite effects caused by Pb and sulphur additions, respectively, one tries to decrease the  $T_c$ , while the other tries to promote it.

## Conclusions:

The present studies lead us to the following conclusion:

- (i) The sample with small concentrations of dopant were largely single phase superconducting materials.
- (ii) Although the effect of PbS doping in YBCO was to decrease the  $T_c$ , it increased the sinterability of the samples at relatively reduced temperatures.
- (iii) There is evidence to suggest that while most of the sulphur substitutes for oxygen, so is not the case with Pb possibly due to the fact that  $Pb^{2+}$  is too large as compared to  $Cu^{2+}$ .
- (iv) The  $T_c$  was generally found to decrease with increasing concentration of PbS in YBCO with the exception of one sample ( $x=0.02$ ).
- (v) The  $\rho(300)$  generally increases as the PbS concentration increases in YBCO.
- (vi) A  $3D \rightarrow 2D$  crossover in superconductivity is observed in the investigated composition range ( $0 \leq x \leq 0.2$ ). The pure sample ( $x=0$ ) was found to be 3D in nature but the samples with  $x > 0.02$  showed a reduced dimensionality of 2.

Table 3.1

X-ray powder diffraction data for  $\text{YBa}_2(\text{Cu}_{1-x}\text{Pb}_x)_3\text{S}_{3x}\text{O}_y$ 

x	Sample code	hkl	2 $\theta$	I/I <sub>0</sub>	d <sub>hkl</sub>	Remarks
0.0	AK02T	003/010	22.8	2.5	3.8969	
		102	27.90	4.5	3.1950	
		013/110/103	32.80	100.0	2.7281	
		014/005	38.60	13.0	2.3305	
		113	40.45	15.0	2.2280	
		006/020	46.76	30.0	1.9410	
		200	47.60	25.0	1.9087	
		115	51.65	5.0	1.7700	
		123/116	58.24	42.0	1.5828	
		213	58.72	41.0	1.5709	
		214/205	62.7	3.0	1.4805	
		026	68.20	8.0	1.3739	
		206/220	68.84	26.0	1.3627	
0.005	AK04T	003/010	22.84	7.0	3.8901	
		102	27.8	5.0	3.2063	
		013/110/103	32.80	100.0	2.7281	
		014/005	38.66	20.0	2.3269	
		113	40.42	13.0	2.2296	
		020/006	46.70	33.0	1.9434	
		200	47.60	20.0	1.9125	
		123/116	58.36	50.0	1.5798	
		213	58.6	36.0	1.5739	
		214/205	62.80	7.0	1.4784	

	026	68.20	8.5	1.3739	
	206/220	68.80	30.00	1.3633	
0.01 AK11T	-	29.6	16.0	3.0153	Y <sub>2</sub> BaCuO <sub>5</sub> Ba <sub>3</sub> Y <sub>4</sub> O <sub>9</sub> ?
	013/110/103	32.8	100.0	2.7281	
	014/005	38.65	24.0	2.3276	
	113	40.43	12.0	2.2291	
	006/020	46.75	35.0	1.9414	
	200	47.5	19.0	1.9125	
	123/116	58.3	47.0	1.5813	
	213	58.66	36.0	1.5725	
	214/205	62.8	5.0	1.4784	
	026	68.2	10.0	1.3739	
	206/220	68.78	26	1.3637	
0.02 AK12T	-	29.5	21.0	3.0253	Ba <sub>3</sub> Y <sub>4</sub> O <sub>9</sub> ? Y <sub>2</sub> BaCuO <sub>5</sub>
	013/110/103	32.8	100.0	2.7281	
	014/005	38.8	24.0	2.3189	
	113	40.4	16.0	2.2306	
	006/020	46.7	25.0	1.9434	
	200	47.5	17.0	1.9125	
	-	52.3	13.0	1.7477	BaPbO <sub>3</sub>
	123/116	58.34	47.0	1.5803	
	213	58.65	38.0	1.5727	
	214/205	62.8	7.0	1.4784	
	026	68.2	10.0	1.3739	
	206/220	68.8	33.0	1.3633	
0.05 AK03T	102	27.8	10.0	3.2063	
	-	29.5	11.0	3.0253	Ba <sub>3</sub> Y <sub>4</sub> O <sub>9</sub>

(Y<sub>2</sub>BaCuO<sub>5</sub>)?

013/110/103	32.8	100.0	2.7281
014/005	38.64	18.0	2.3281
113	40.4	15.0	2.2306
006/020	46.75	29.0	1.9414
200	47.5	20.0	1.9125
-	52.72	5.0	1.7348
123/116	58.34	47.0	1.5803
213	58.7	40.0	1.5715
026	68.2	7.0	1.3739
206/220	68.84	27.0	1.3627

BaPbO<sub>3</sub>

0.08 AK15T

-

29.5 38.0 3.0253 Ba<sub>3</sub>Y<sub>4</sub>O<sub>9</sub>(Y<sub>2</sub>BaCuO<sub>5</sub>)?

013/110/103	32.85	100.0	2.7240
014/005	38.85	23.0	2.3160
113	40.4	14.0	2.2306
006/020	47.0	18.0	1.9317
200	47.3	17.0	1.9201
	52.4	22.0	1.7446
123/116/213	58.5	43.0	1.5764
026/206/220	68.85	28.0	1.3625

BaPbO<sub>3</sub>

0.1 AK16T

-

29.5 56.0 3.0253 Ba<sub>3</sub>Y<sub>4</sub>O<sub>9</sub>(Y<sub>2</sub>BaCuO<sub>5</sub>)?

013/110/103	32.78	100	2.7297
014/005	38.8	23.0	2.3189
113	40.45	14.0	2.2280
-	42.3	25.0	2.1342

Cu<sub>2</sub>Y



006/020	46.9	18.0	1.9356	
200	47.25	24.0	1.9220	
-	52.28	34.0	1.7483	BaPbO <sub>3</sub>

123/116/213	58.54	35.0	1.5753	
026/206/220	68.9	24.0	1.3616	Ba <sub>2</sub> PbO <sub>4</sub> ?

0.2 AK17T

-	21.1	11.0	4.1870	.
-	29.5	100.0	3.0253	Ba <sub>2</sub> Y <sub>4</sub> O <sub>9</sub> (Y <sub>2</sub> BaCuO <sub>5</sub> )
013/110/103	32.8	28.0	2.7281	
-	35.6	11.0	2.5197	
014/005	38.94	28.0	2.3105	
	42.32	24.0	2.1356	BaPbO <sub>3</sub>
	43.00	21.0	2.1016	Y <sub>2</sub> O <sub>3</sub>
	45.6	9.0	1.9317	Cu <sub>2</sub> Y
006/020/200	47.0	9.0	1.9877	(Y <sub>2</sub> O <sub>3</sub> )?
	52.3	59.0	1.7477	BaPbO <sub>3</sub>
123/116/213	58.45	16.0	1.5776	
	61.28	19.0	1.5114	
026/206/220	69.0	18.0	1.3599	(Ba <sub>2</sub> PbO <sub>4</sub> )
	69.54	22.0	1.3506	Cu <sub>2</sub> Y

Table 3.2

Relative intensities of main impurity phases as a function of doping

Impurity Phase	Doping 'x'	Sample Code	Relative Intensity (%)
$\text{Y}_2\text{BaCuO}_5$ ( $\text{Ba}_3\text{Y}_2\text{O}_9$ )?	0.00	AK02T	5.00
	0.005	AK04T	7.00
	0.01	AK11T	16.00
	0.02	AK12T	21.00
	0.05	AK03T	11.00
	0.08	AK15T	38.00
	0.1	AK16T	56.00
	0.2	AK17T	100.00
$\text{BaPbO}_3$	0.00	AK02T	0.00
	0.005	AK04T	0.00
	0.01	AK11T	0.00

cont/-

---

Impurity Phase	Doping 'x'	Sample Code	Relative Intensity (%)
-------------------	---------------	----------------	---------------------------

---

	0.02	AK12T	13.00
	0.05	AK03T	05.00
	0.08	AK15T	22.00
	0.1	AK16T	34.00
	0.2	AK17T	59.00

---

Table 3.3

Room temperature resistivities ( $\rho(300)$ ), transition temperature ( $T_c$ ) and transition widths ( $\Delta T_c$ ) for the superconducting oxides  $\text{YBa}_2(\text{Cu}_{1-x}\text{Pb}_x)_3\text{S}_{3-x}\text{O}_y$ .

composition (x)	Sample code	$\rho(300)$ ( $10^{-5} \Omega\text{m}$ )	$\left[\frac{dp}{dT}\right]_N^+$ ( $10^{-3} \Omega\text{m/K}$ )	$T_c$ (K)	Transition width ( $\Delta T_c$ ) (K)
0.00	AK02T	2.41	1.86	90.2	2.0
0.005	AK04T	2.60	1.76	87.2	2.2
0.01	AK11T	2.93	1.54	85.8	0.8
0.02	AK12T	3.67	2.35	86.75	1.5
0.05	AK03T	2.33	1.58	85.4	1.9
0.08	AK15T	17.98	*	78.0	> 2
0.10	AK16T	97.13	*	59.0	> 2

\*  $dp/dT$  is negative and continuously changing (semiconductor-like).

+  $\langle dp/dT \rangle_N$  is calculated from the  $\rho$  vs  $T$  linear plot in the temperature range  $1.5 T_c \leq T \leq 300\text{K}$ .

Table 3.4

Superconducting order parameter and characteristic length parameter as a function of doping (x) in  $\text{YBa}_2(\text{Cu}_{1-x}\text{Pb}_x)_3\text{S}_{3-x}\text{O}_y$ .

Fractional substitution x	Sample Code	Order Parameter n	Characteristic Length parameter K
0.00	AK02T	-0.5042	315.7968
0.005	AK04T	-0.3609	248.0781
0.01	AK11T	-0.4826	284.5666
0.02	AK12T	-0.9706	525.4234
0.05	AK03T	-0.9997	538.6190

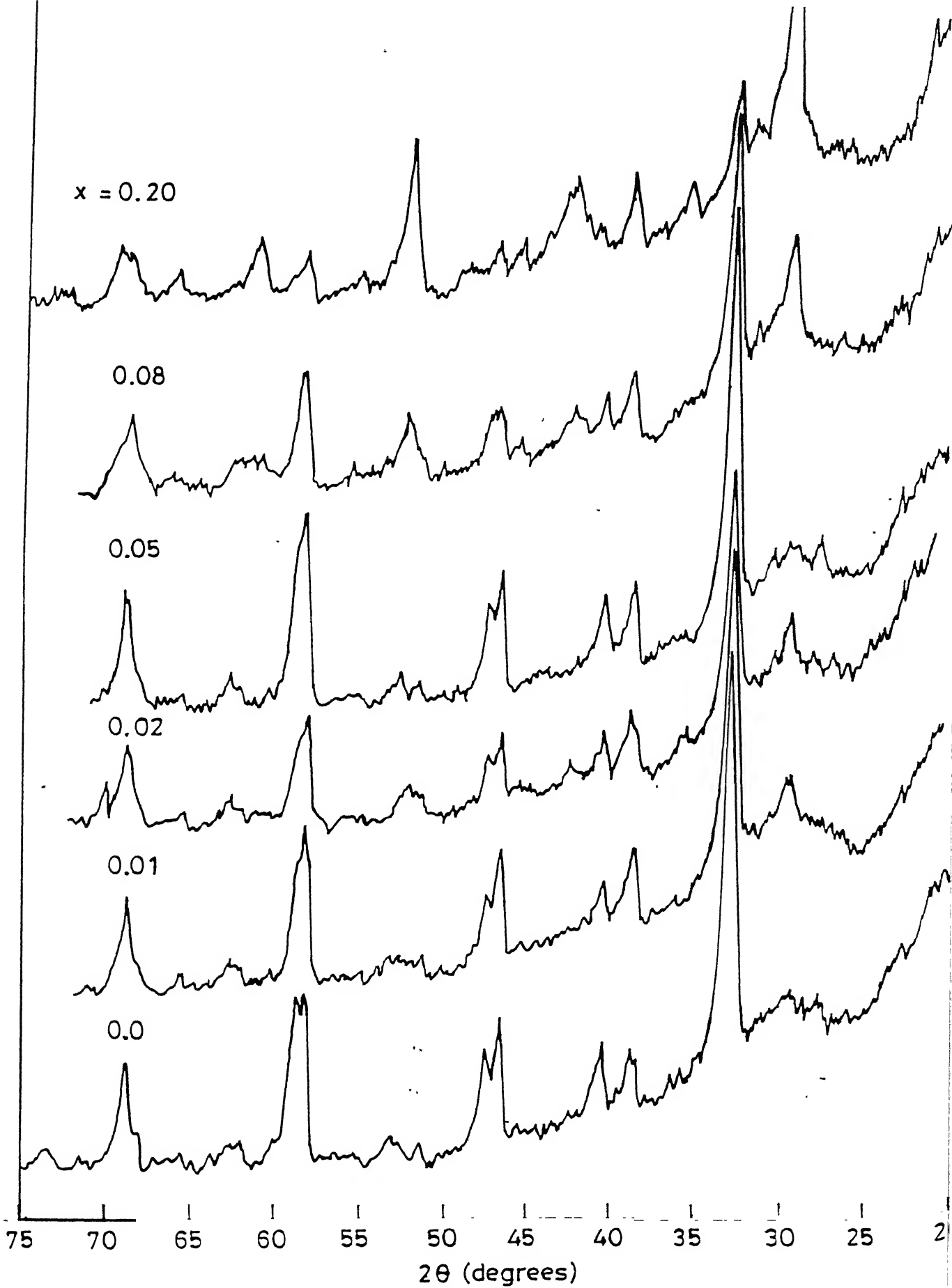


FIG.3-1: X-RAY DIFFRACTION PATTERNS FOR  $\text{YBa}_2(\text{Cu}_{1-x}\text{Pb}_x)_3\text{S}_{3x}\text{O}_y$







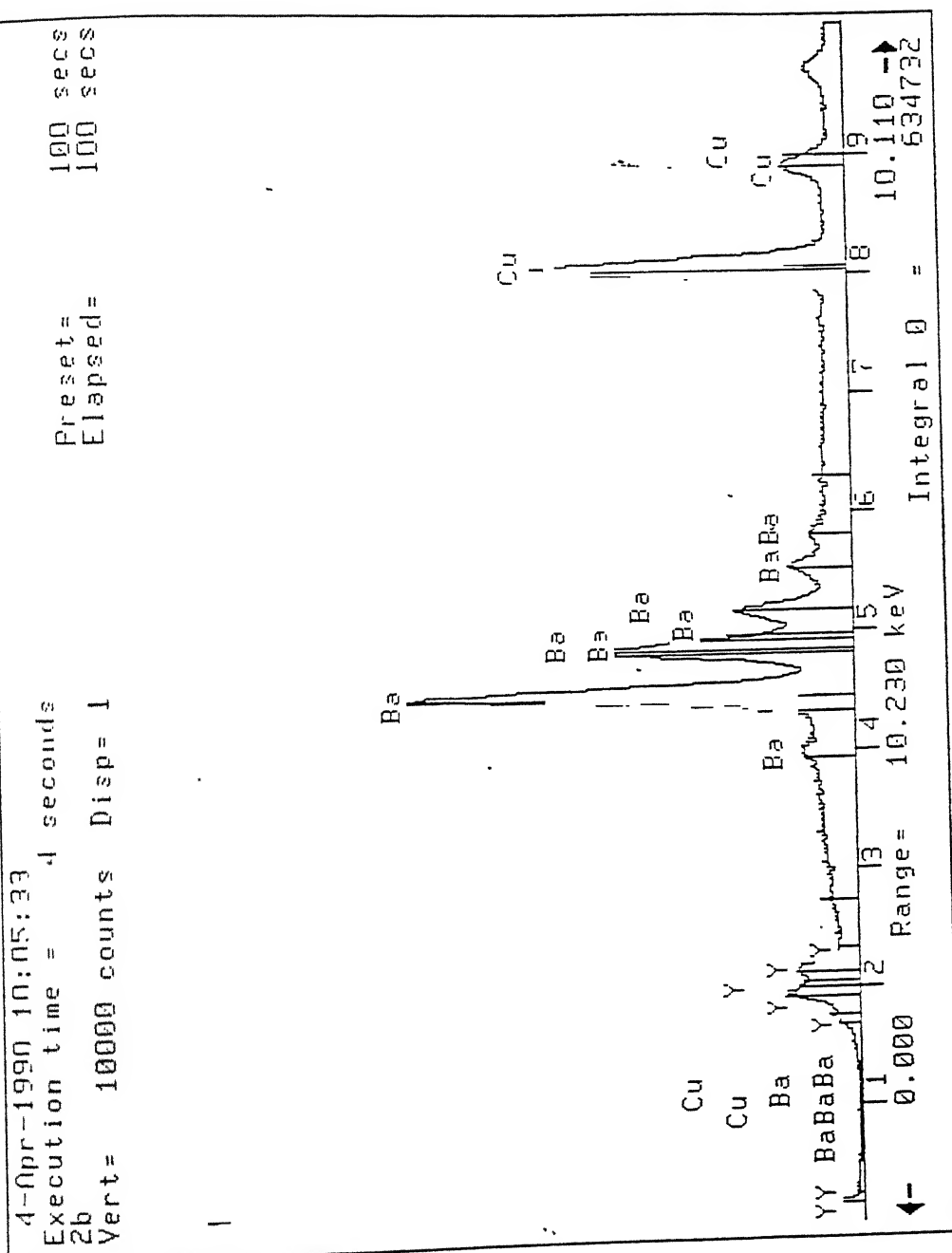
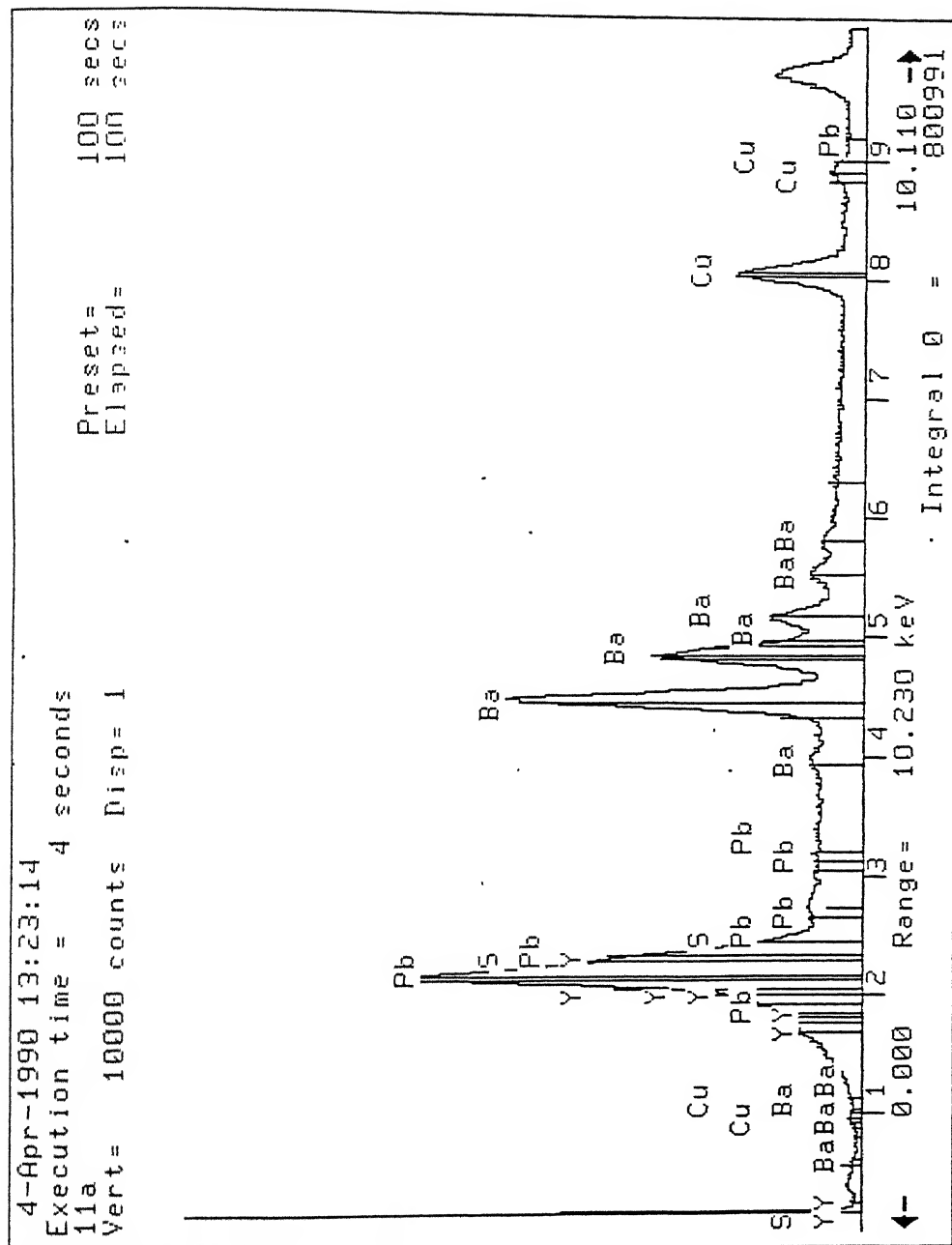


FIG.3.4: EDX-SPECTRUM SHOWING THE SECOND [GRAY] IMPURITY PHASE RICH IN Ba AND Cu.



**FIG.3.5: EDX-SPECTRUM SHOWING THE SECOND [GRAY] IMPURITY PHASE RICH IN Ba AND Pb.**

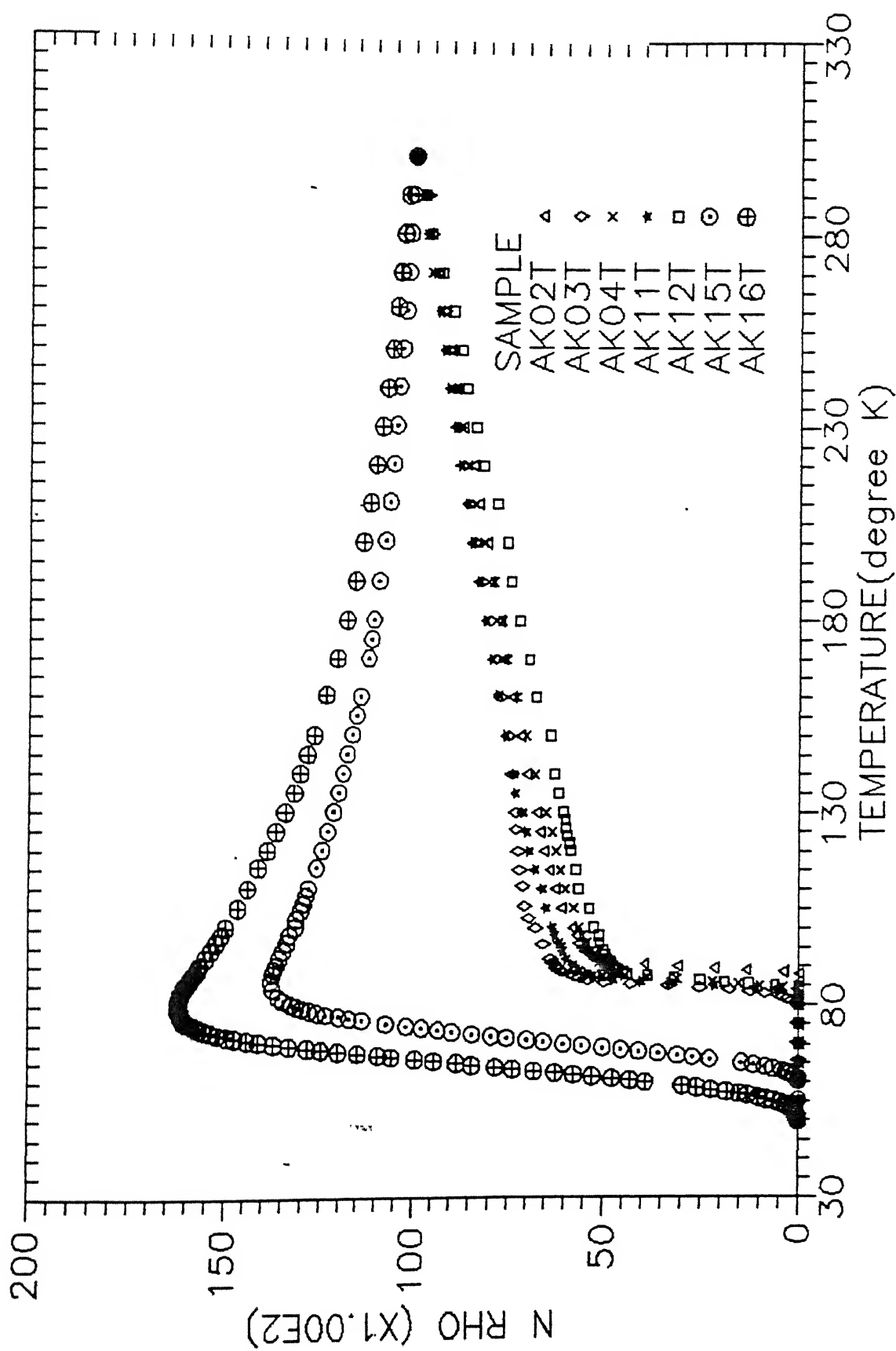


FIG.3.6 :NORMALIZED RESISTIVITY VS. TEMPERATURE PLOTS FOR PbS DOPED YE

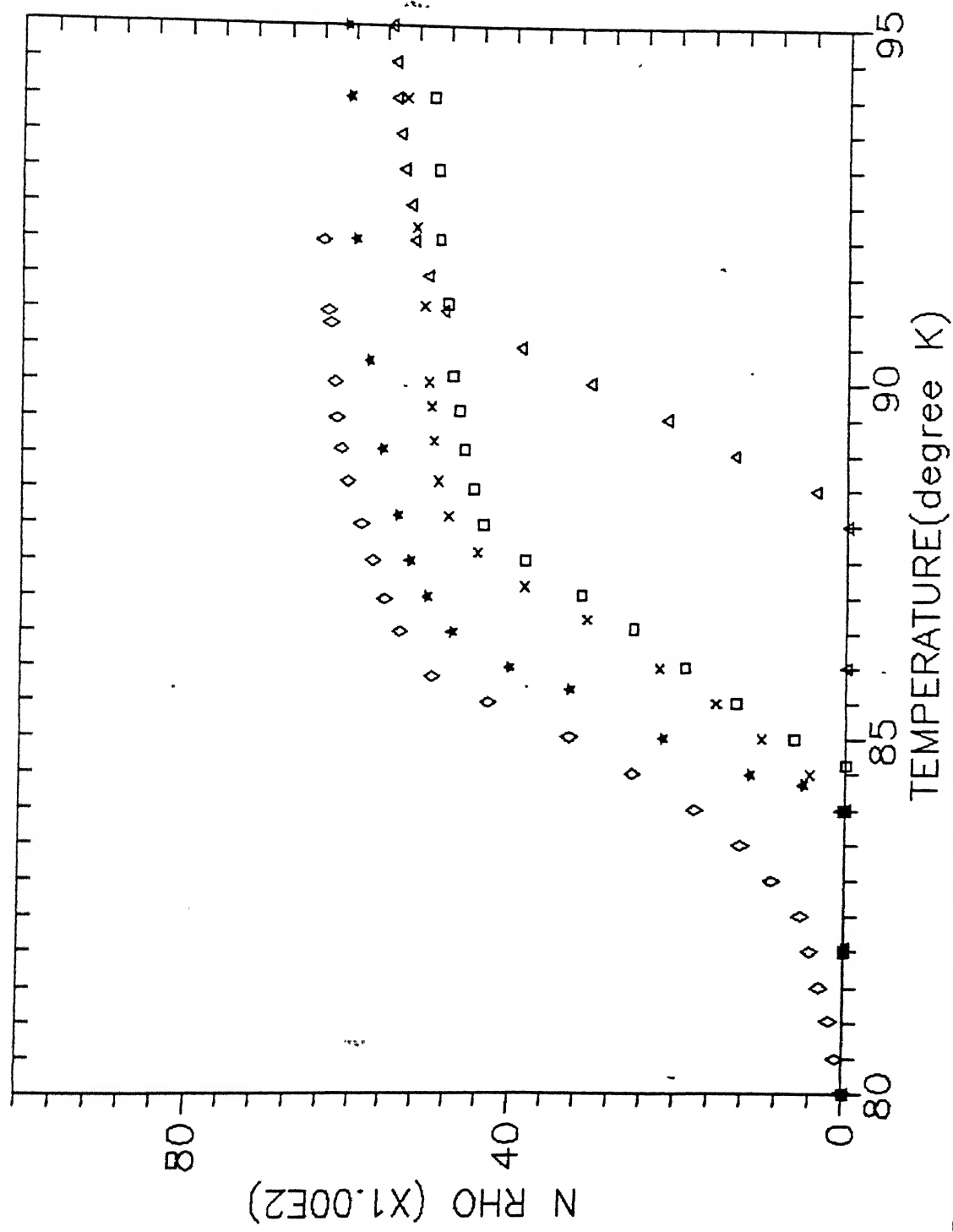


FIG.3.7 :TRANSITION REGIONS OF THE PbS DOPED YBCO--SUPERCONDUCTORS

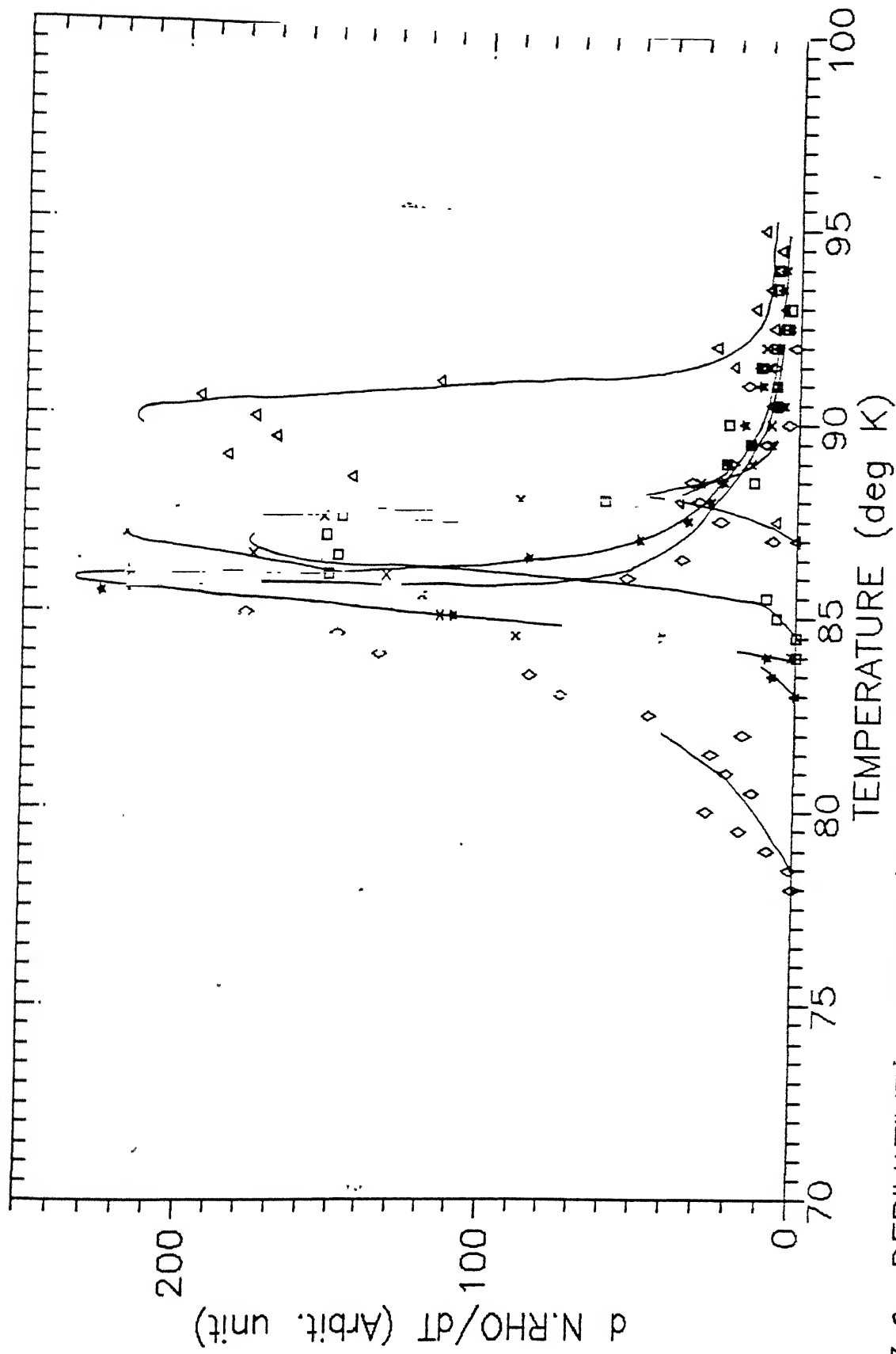


FIG.3.8 :DERIVATIVE  $d N.RHO/dT$  VS. TEMPERATURE FOR PbS DOPED YBCO

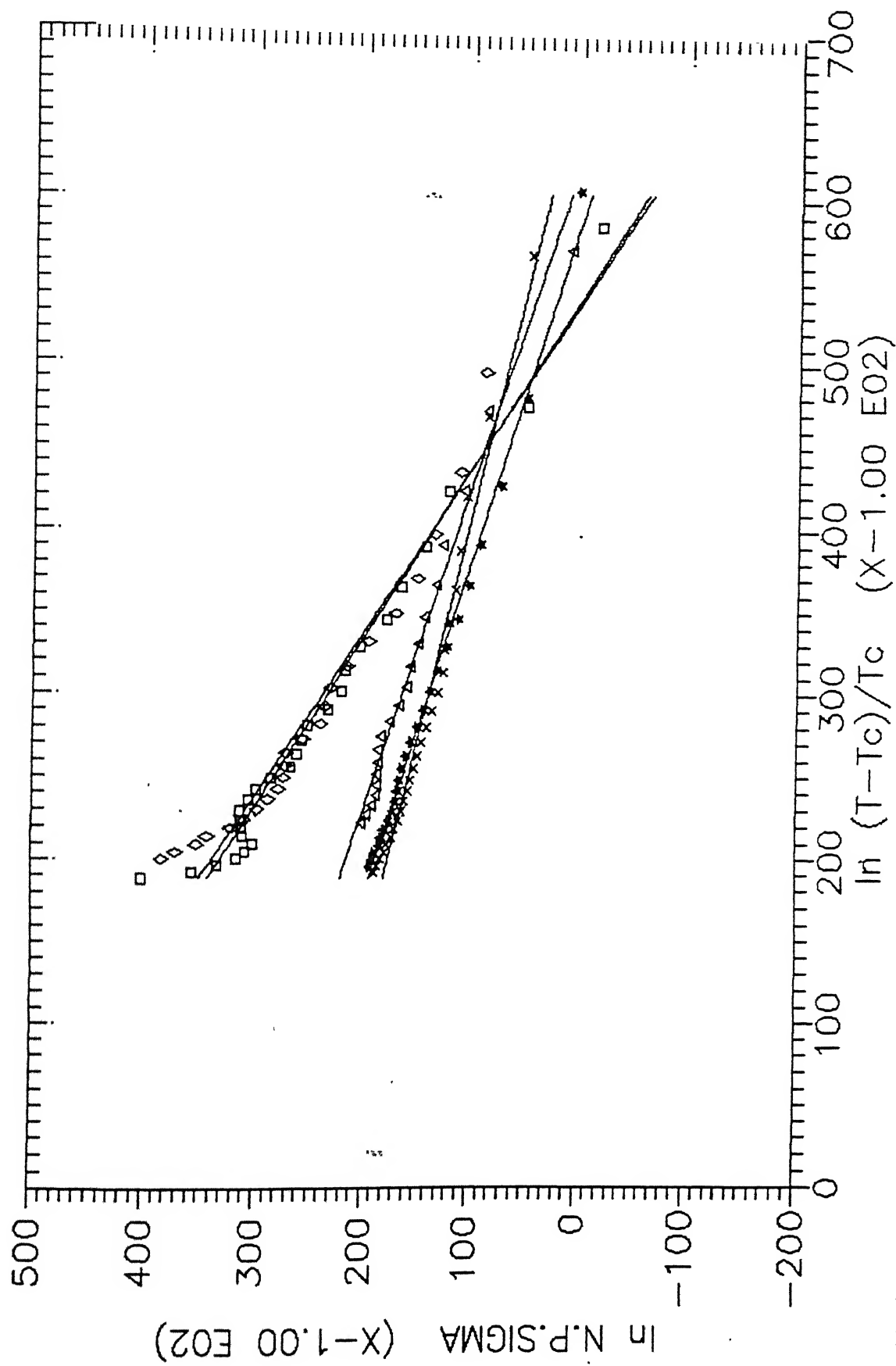


FIG.3.9 :PARACONDUCTIVITY VS. REDUCED TEMPERATURE FOR PbS DOPED YBCO

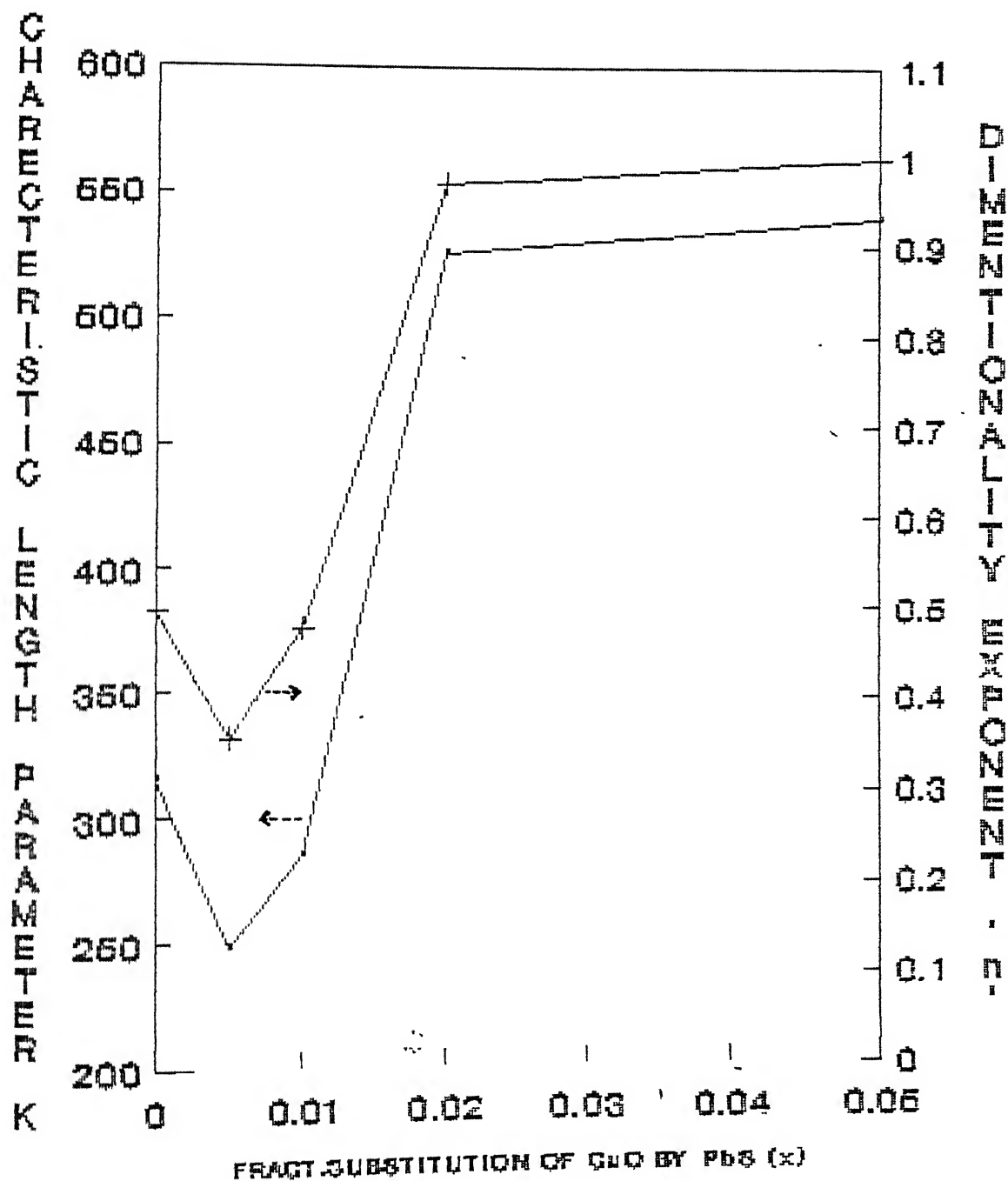


FIG. 3.10: CHARACTERISTIC PARAMETERS FOR PbS DOPED YBCO HIGH  $T_c$  SUPERCONDUCTOR

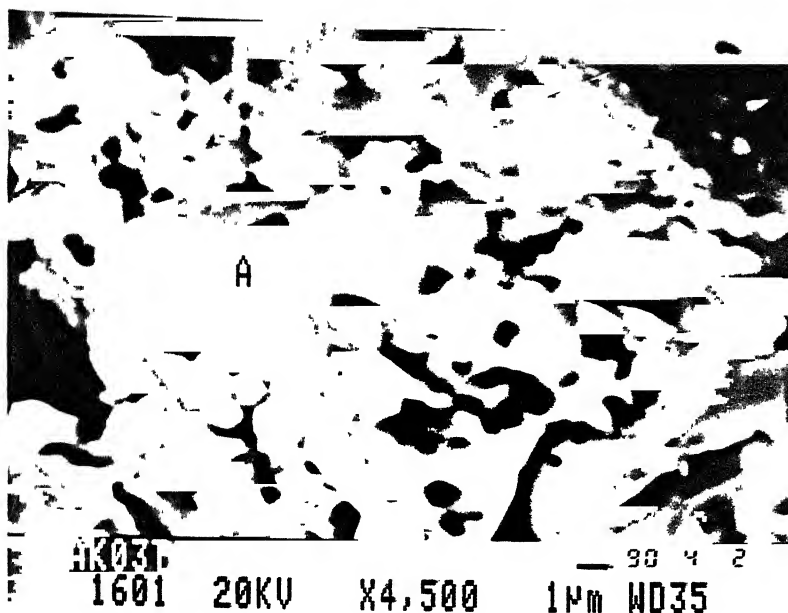


PLATE 3.3: SEM-MICROPHOTOGRAPH FOR THE  
SAMPLE AK03T [ $x=0.1$ ]

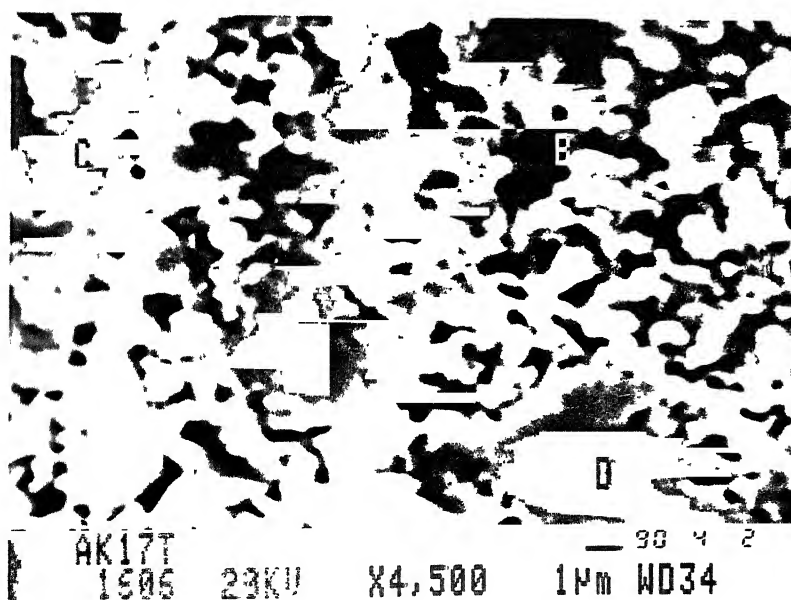


PLATE 3.4: SEM-MICROPHOTOGRAPH FOR THE  
SAMPLE AK17T [ $x=0.2$ ] SHOWING  
A DECREASE IN GRAIN SIZE



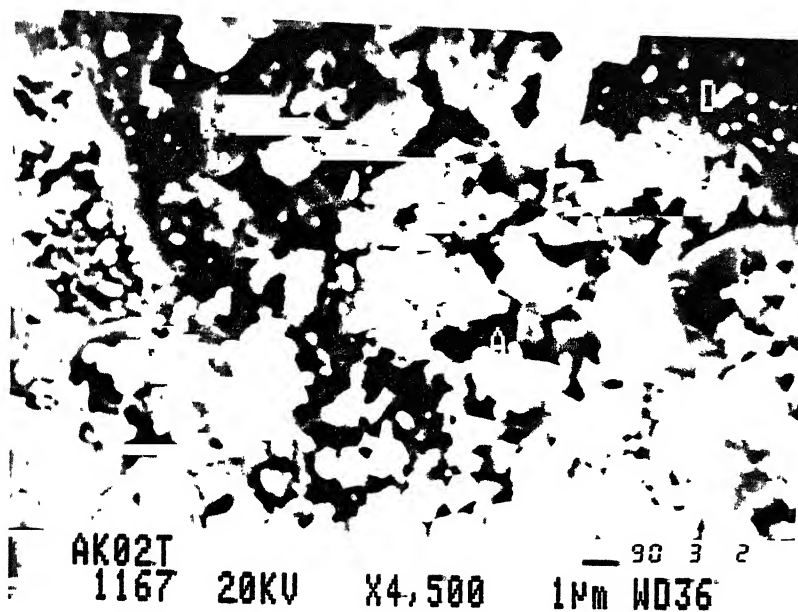


PLATE 3.1: SEM-MICROPHOTOGRAPH FOR THE SAMPLE AK02T [ $x=0$ ].

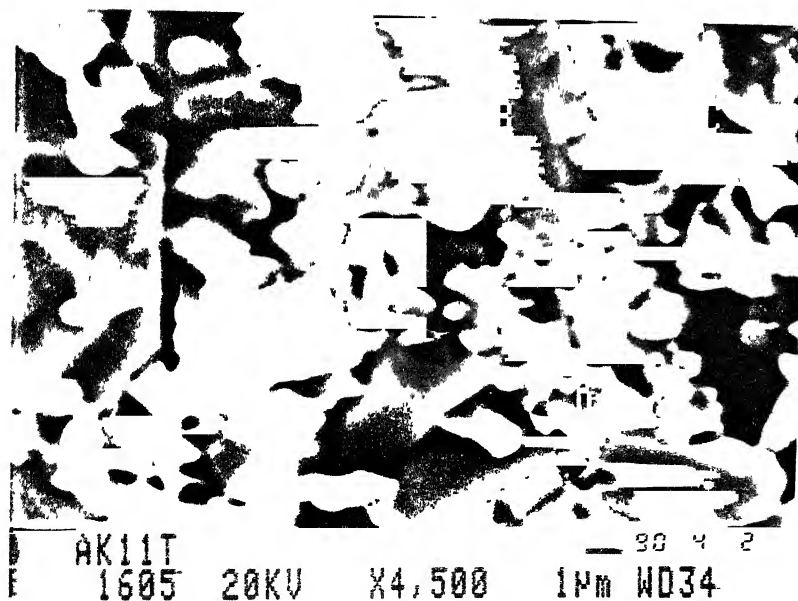


PLATE 3.2: SEM-MICROPHOTOGRAPH FOR THE SAMPLE AK11T [ $x=0.02$ ] SHOWING AN INCREASE IN GRAIN SIZE

## References

1. Ki Hyun Yoon, Shung Sik Chang, J. Appl. Phys. 67(5), 2516 1990.
2. A.J. Jacobson, J.M. Newsam, D.C. Johnston, J.P. Stokes, S. Bhattacharya, J.T. Lewandowski, D.P. Goshorn, M.J. Higgins, M.S. Alvarez, in "Chemistry of oxide superconductors", Ed. C.N.R. Rao p-43, 1988.
3. Y. Nakazawa, M. Ishikawa, T. Takabatake, H. Takeya, T. Shibuya, K. Terakura, F. Takei, Jpn. J. Appl. Phys. 26(5), L682, 1987.
4. K. Takagi, K. Miyauchi, T. Ito, T. Aida, H. Hasegawa, U. Kowabe Jpn. J. Appl. Phys. 26(5), L699, 1987.
5. Y. Matsumoto, T. Abe, M. Tanaka, T. Tajawa, E. Sato, Mat. Res. Bull. 23, 1241, 1988.
6. Xia Jiansheng, Cao Liezhao, Fang Minghu, Zhang Dirui, Zhang Han, Qian Yitai, Solid Stat. Comm. 68(7), 643, 1988.
7. J. Langer, M. Veit, M. Galfy, H.D. Jostarndt, A. Erie, S. Blumenroder, H. Schmidt, E. Zirngiebl, Solid Stat. Comm. 65, 973, 1988.
8. G. Xio, C.M. Cieplak, A. Gravin, F.H. Streitz, A. Bakhsai, C.L. Chien, Phys. Rev. Lett. 60, 1446, 1988.
9. X. Jiasheng, Chin. J. Low Temp. Phys. 11(5), 353, 1989.
10. K.N.R. Taylor, D.N. Matthews, G.J. Russell, J. Cryst. growth 85, 628, 1987.
11. S. Kambe and M. Kawai, Jpn. J. Appl. Phys. 27(12), L2342, 1988.
12. A.S. Bhalla, R. Roy, L.E. Cross, in "Chemistry of oxide superconductors" Ed. C.N.R. Rao, p-71, 1988.
13. A.F. Hepp., J.R. Gaier, P.D. Hambourger, J.J. Pouch, in "Processing and Applications of High T<sub>c</sub> superconductors", Ed. W.E. Mayo, The Metallurgical Society, p-213, 1988.
14. R. Wodenweber, H.U. Krebs, F. Gelsdorf, K. Heinemann, G.V.S. Sastry, H.C. Treyhardt, K. Winzer Appl. Phys. Lett. 52(4), 317, 1988.
15. F. Stucki, P. Bruesch, T. Baumann, Physica C 153-155, 200, 1988.
16. M.R. Harrison, I.C.S. Hegedus, W.G. Freeman, in "Chemistry

17. D.Y. Xing, Z.D. Wang, C.D. Gong, Z. Phys. B Cond. Matt. 77, 61, 1989.
18. B.A. Recherts, R.E. Allen, Phy. Rev. B37, 7496, 1987.
19. J.M. Trascon, P. Barboux, P.F. Micelli, L.H. Greens, G.W. Hull, M. Eibschultz, S.A. Sunshine, Phys. Rev. B37, 7458, 1988.
20. G. Baumgartel, K.H. Bennemann, Phy. Rev. B40 (10), 6711, 1989.
21. N.P. Bansal, D. Boyne, D.E. Farrell, J. Superconductivity 1(4), 417, 1988.
22. Y.D. Rao, A. Krol, Y.H. Rao, C. Walters, S. Spagna, J. Althoff, S. Woronick, L.Y. Jang, F.Xu, Mat. Res. Soc. Symp. Proc. 99, 407, 1988.
23. D. Shindo, K. Hiraga, M. Hirabayashi, A. Tokiwa, M. Kikuchi, Y. Syono, O. Nakatsu, N. Kobayashi, Y. Muto, E. Aoyagi, Jpn. J. Appl. Phys. 26(10), L1667, 1987.
24. Y. Maeno, T. Fujita, Proc. Int. Workshop Novel Mechanism of Superconductivity July 1987 Berkeley Calif. (Plenum Press N.Y.) 1988.
25. S.J. Hagen, Z.Z. Wang, N.P. Ong, Phy. Rev. B 38(10), 7137, 1988.
26. Deutscher, in "Novel Superconductivity" Ed. S.A. Wolf V.Z. Kresin (Plenum) p. 293, 1987.
27. P.P. Freitas, C.C. Tsuei, T.S. Plaskett, Phy. Rev. B36(1) 833, 1987.
28. V.L. Ginsburg, L.D. Landau, JEPT 20, 1064, 1950.
29. W.J. Skocpol, M.Tinkham, Rep. Prog. Phys. 38, 1049, 1975.
30. M. Hikita, M. Suzuki, Phys. Rev. B 41(1), 834, 1990.
31. F. Vidal, J.A. Veira, J. Maza, J.J. Ponte, Physica 156 807, 1988.
32. G. Weigang, K. Winzev, Z. Phy. B. Cond. Matt., 77, 11 1989.
33. A. Schulte, G. Fritsch, E. Luscher, Z. Phy. B Cond. Matt 78, 457, 1990.
34. S. Hikami, A.I. Larkin, Mod. Phys. Lett. B2, 693, 1988.
35. K. Maki, R.S. Thomson, Phys. Rev. B39, 2767, 1989.

- 36. A.G. Aronov, S. Hikami, A.I. Larkin, *Phy. Rev. Lett.* 62, 965, 1989
- 37. S.P. Muntyan, G.A. Kioss, F.M. Muntyanu.  
*Phy. Stat. Solidi A* 114, 1, pk-63, 1989.
- 38. L. Palhan, A. Brokman, T. Felner, M. Brettschneider, Y. Yacoby, M. Weger, *Solid Stat. Comm.* 68(3), 313, 1988.
- 39. I. Felner, B. Barbara, *Phys. Rev.* 37(10), 5820, 1988.

TH  
620.112 973

**A108883**

## Date Slip

Y 952a

1952a  
This book is to be returned on the  
date last stamped.

[illegible]

S-1990-M-TYA-ADV